

University of Groningen

Water in bacterial biofilms

Quan, Kecheng; Hou, Jiapeng; Zhang, Zexin; Ren, Yijin; Peterson, Brandon W.; Flemming, Hans-Curt; Mayer, Christian; Busscher, Henk J.; van der Mei, Henny C.

Published in:
Critical Reviews in Microbiology

DOI:
[10.1080/1040841X.2021.1962802](https://doi.org/10.1080/1040841X.2021.1962802)

IMPORTANT NOTE: You are advised to consult the publisher's version (publisher's PDF) if you wish to cite from it. Please check the document version below.

Document Version
Publisher's PDF, also known as Version of record

Publication date:
2022

[Link to publication in University of Groningen/UMCG research database](#)

Citation for published version (APA):

Quan, K., Hou, J., Zhang, Z., Ren, Y., Peterson, B. W., Flemming, H-C., Mayer, C., Busscher, H. J., & van der Mei, H. C. (2022). Water in bacterial biofilms: pores and channels, storage and transport functions. *Critical Reviews in Microbiology*, 48(3). <https://doi.org/10.1080/1040841X.2021.1962802>

Copyright

Other than for strictly personal use, it is not permitted to download or to forward/distribute the text or part of it without the consent of the author(s) and/or copyright holder(s), unless the work is under an open content license (like Creative Commons).

The publication may also be distributed here under the terms of Article 25fa of the Dutch Copyright Act, indicated by the "Taverne" license. More information can be found on the University of Groningen website: <https://www.rug.nl/library/open-access/self-archiving-pure/taverne-amendment>.

Take-down policy

If you believe that this document breaches copyright please contact us providing details, and we will remove access to the work immediately and investigate your claim.

Downloaded from the University of Groningen/UMCG research database (Pure): <http://www.rug.nl/research/portal>. For technical reasons the number of authors shown on this cover page is limited to 10 maximum.



Water in bacterial biofilms: pores and channels, storage and transport functions

Kecheng Quan, Jiapeng Hou, Zexin Zhang, Yijin Ren, Brandon W. Peterson, Hans-Curt Flemming, Christian Mayer, Henk J. Busscher & Henny C. van der Mei

To cite this article: Kecheng Quan, Jiapeng Hou, Zexin Zhang, Yijin Ren, Brandon W. Peterson, Hans-Curt Flemming, Christian Mayer, Henk J. Busscher & Henny C. van der Mei (2022) Water in bacterial biofilms: pores and channels, storage and transport functions, *Critical Reviews in Microbiology*, 48:3, 283-302, DOI: [10.1080/1040841X.2021.1962802](https://doi.org/10.1080/1040841X.2021.1962802)

To link to this article: <https://doi.org/10.1080/1040841X.2021.1962802>



© 2021 The Author(s). Published by Informa UK Limited, trading as Taylor & Francis Group.



Published online: 19 Aug 2021.



[Submit your article to this journal](#)



Article views: 1908



[View related articles](#)






[View Crossmark data](#)



Citing articles: 3 [View citing articles](#)

Water in bacterial biofilms: pores and channels, storage and transport functions

Kecheng Quan^{a,b*}, Jiapeng Hou^{a*} , Zexin Zhang^b, Yijin Ren^c , Brandon W. Peterson^a, Hans-Curt Flemming^{d,e}, Christian Mayer^f, Henk J. Busscher^a and Henny C. van der Mei^a 

^aDepartment of Biomedical Engineering, University of Groningen and University Medical Center Groningen, Groningen, The Netherlands; ^bCollege of Chemistry, Chemical Engineering and Materials Science, Soochow University, Suzhou, P.R. China; ^cDepartment of Orthodontics, University of Groningen and University Medical Center Groningen, Groningen, The Netherlands; ^dSingapore Centre for Environmental Life Sciences/Engineering and the School of Biological Sciences, Nanyang Technological University, Singapore, Singapore; ^eFaculty of Chemistry, Biofilm Centre, University of Duisburg-Essen, Essen, Germany; ^fFaculty of Chemistry, Physical Chemistry, University of Duisburg-Essen, Essen, Germany

ABSTRACT

Bacterial biofilms occur in many natural and industrial environments. Besides bacteria, biofilms comprise over 70 wt% water. Water in biofilms occurs as bound- or free-water. Bound-water is adsorbed to bacterial surfaces or biofilm (matrix) structures and possesses different Infra-red and Nuclear-Magnetic-Resonance signatures than free-water. Bound-water is different from intra-cellularly confined-water or water confined within biofilm structures and bacteria are actively involved in building water-filled structures by bacterial swimmers, dispersion or lytic self-sacrifice. Water-filled structures can be transient due to blocking, resulting from bacterial growth, compression or additional matrix formation and are generally referred to as “channels and pores.” Channels and pores can be distinguished based on mechanism of formation, function and dimension. Channels allow transport of nutrients, waste-products, signalling molecules and antibiotics through a biofilm provided the cargo does not adsorb to channel walls and channels have a large length/width ratio. Pores serve a storage function for nutrients and dilute waste-products or antimicrobials and thus should have a length/width ratio close to unity. The understanding provided here on the role of water in biofilms, can be employed to artificially engineer by-pass channels or additional pores in industrial and environmental biofilms to increase production yields or enhance antimicrobial penetration in infectious biofilms.

ARTICLE HISTORY

Received 12 March 2021
Revised 17 June 2021
Accepted 21 July 2021
Published online 18 August 2021

KEYWORDS





Pores in biofilms; channels in biofilms; diffusion; extracellular polymeric substances; bound water; free water; transport in a biofilm

Introduction

Bacterial biofilms are defined as communities of surface-adhering and surface-adapted bacteria, growing in a self-produced matrix of extracellular polymeric substances (EPS) (Tolker-Nielsen 2015) and occurring in virtually all industrial and natural environments, including the human body. Although this definition may give the impression that bacteria form the main constituents of a biofilm, volumetric bacterial densities in a biofilm are low between 0.2 and 0.4 bacteria μm^{-3} (Roberts and Stewart 2004; Gusnaniar et al. 2017), corresponding with volume fractions ranging from 0.1 to 0.2. Water actually is the most prevalent component in a biofilm by weight (see Table 1) and volume, leaving only 1–2%

available for bacteria in a biofilm and the remainder to EPS matrix components. Exact percentages depend on the type of biofilm considered. To emphasise the importance of water in biofilms, Marshall has suggested “stiff water” as a nickname for biofilms (Flemming and Wingender 2010).

Water is essential for life in a biofilm. It maintains osmotic pressure, dissolves nutrient molecules and provides a medium for macromolecular transport and functioning (Galdino et al. 2020). Although bacteria need water to grow, they are at the same time, able to survive storage after freeze-drying for extended periods of time (Coulibaly et al. 2010). However, in general water activities less than 0.60 inactivate protein function

CONTACT Zexin Zhang  zhangzx@suda.edu.cn  College of Chemistry, Chemical Engineering and Materials Science, Soochow University, Ren'ai road 199, Suzhou 215123, P.R. China; Henny C. van der Mei  h.c.van.der.mei@umcg.nl  Department of Biomedical Engineering, University of Groningen and University Medical Center Groningen, FB-40, Antonius Deusinglaan 1, 9713 AV Groningen, The Netherlands

*Both first authors contributed equally.

© 2021 The Author(s). Published by Informa UK Limited, trading as Taylor & Francis Group.

This is an Open Access article distributed under the terms of the Creative Commons Attribution-NonCommercial-NoDerivatives License (<http://creativecommons.org/licenses/by-nc-nd/4.0/>), which permits non-commercial re-use, distribution, and reproduction in any medium, provided the original work is properly cited, and is not altered, transformed, or built upon in any way.

Table 1. Water content by weight in biofilms of different bacterial strains.

Bacterial strain	Water content (wt%)	Technique	Reference
<i>Bacillus subtilis</i>	89	120 °C oven drying	(Bratbak and Dundas 1984)
<i>Escherichia coli</i>	77	120 °C oven drying	(Bratbak and Dundas 1984)
<i>Pseudomonas aeruginosa</i>	88–92	Confocal RM ^a	(Sandt et al. 2008)
<i>Pseudomonas putida</i>	81	120 °C oven drying	(Bratbak and Dundas 1984)
<i>Pseudoalteromonas</i> sp.	87–94	Confocal RM	(Sandt et al. 2009)
<i>Streptococcus mutans</i>	70–75	RM	(Sandt et al. 2009)
<i>Streptococcus mutans</i>	84	80 °C oven drying	(Tam et al. 2007)
<i>Sphingomonas</i> sp.	97	105 °C oven drying	(Zhang et al. 1998)
Activated sewage sludge	Up to 98	105 °C oven drying	(Chan and Wang 2016)

^aRaman microspectroscopy.

(Tarek and Tobias 2002; Esbelin et al. 2018) and break DNA double-strands (Mattimore and Battista 1996) in bacteria, leading to cell death within days (meningococci (Tzeng et al. 2014)) to months (deinococci (Mattimore and Battista 1996)). Arguably, near-complete desiccation may be more of a challenge to deal with for biofilms in many environments than total loss of water causing complete metabolic arrest. During total dehydration of a biofilm, water as a transport medium for nutrients, waste-products and other molecules is no longer needed in full absence of metabolic processes, opposite as during near-complete dehydration (Decho 2017). Desiccated *Deinococcus geothermalis* biofilms even remained viable for almost 2 years when exposed on the outside of the international space station (ISS) (Panitz et al. 2019). Apart from the known protection against mechanical and chemical attacks offered to bacteria in their biofilm-mode of growth, biofilms are characterised by water-filled regions (Figure 1) to protect its inhabitants against desiccation (Esbelin et al. 2018) and support storage and transport of nutrients and waste products through a biofilm. Effects of dehydration and rehydration have both been extensively studied with respect to bacterial cells (Rapoport et al. 2019). However, this is not true for water in the immediate environment of a bacterial cell (Decho 2017). In a biofilm, the immediate environment of a bacterial cell is the EPS matrix. Important functions of water in biofilms are largely understudied compared to, for instance the role of EPS or bacteria themselves in a biofilm. Therefore, this review focuses on how water in immersed, wetted or dried biofilm can be affirmatively demonstrated, distinguishing different structural features of biofilm regions in which water is retained and the functions that water-filled regions fulfil in a biofilm.

Water-filled regions in biofilms-bound versus free water

There are several techniques available that allow to visualise open structures in biofilms that are generally assumed to be water-filled. Fewer techniques are

available that provide affirmative evidence of water presence in biofilm regions and also allow quantification of water in biofilms (see Table 2 for a comprehensive summary). The forthcoming sections will first focus on visualisation techniques and subsequently describe techniques that provide evidence for the presence of water in biofilms and the quantification of the amount of water in biofilms.

Visualisation of assumed water-filled regions in a biofilm

Many techniques said to demonstrate water-filled regions in biofilms, in fact only visualise bacterial clusters in biofilms together with open structures that are assumed to be water-filled without affirmative evidence of the presence of water. Light source-based microscopy, like e.g. Confocal Laser Scanning Microscopy (CLSM) has a higher spatial resolution than e.g. NMR-based techniques (see Table 2), but does not directly and affirmatively confirm water presence. However, using CLSM on stained biofilms, flow of injected 0.3 µm diameter fluorescent particle suspensions in water through biofilms has been visualised (Stoodley 1994). Particles did not penetrate through bacterial clusters, indicating absence of water-filled regions that are large enough to allow particle passage. Smaller fluorescent dyes however, have been demonstrated to penetrate through bacterial clusters in biofilms after micro-injection (De Beer et al. 1997; Bryers and Drummond 1998; Waharte et al. 2010).

Electron microscopy, similar to light source-based microscopy, does not directly and affirmatively identify water, but instead is able to show dewatered, collapsed biofilm structures with a nanoscopic resolution, assumed to be water-filled prior to biofilm preparation for microscopy purposes. Moreover, the high vacuum conditions required for most types of electron microscopy inevitably will give rise to drying artefacts, unless applied in an environmental mode (see Figure 1(D)) that preserves hydration of the biofilm to be imaged (Fernández-Delgado et al. 2015, 2016).

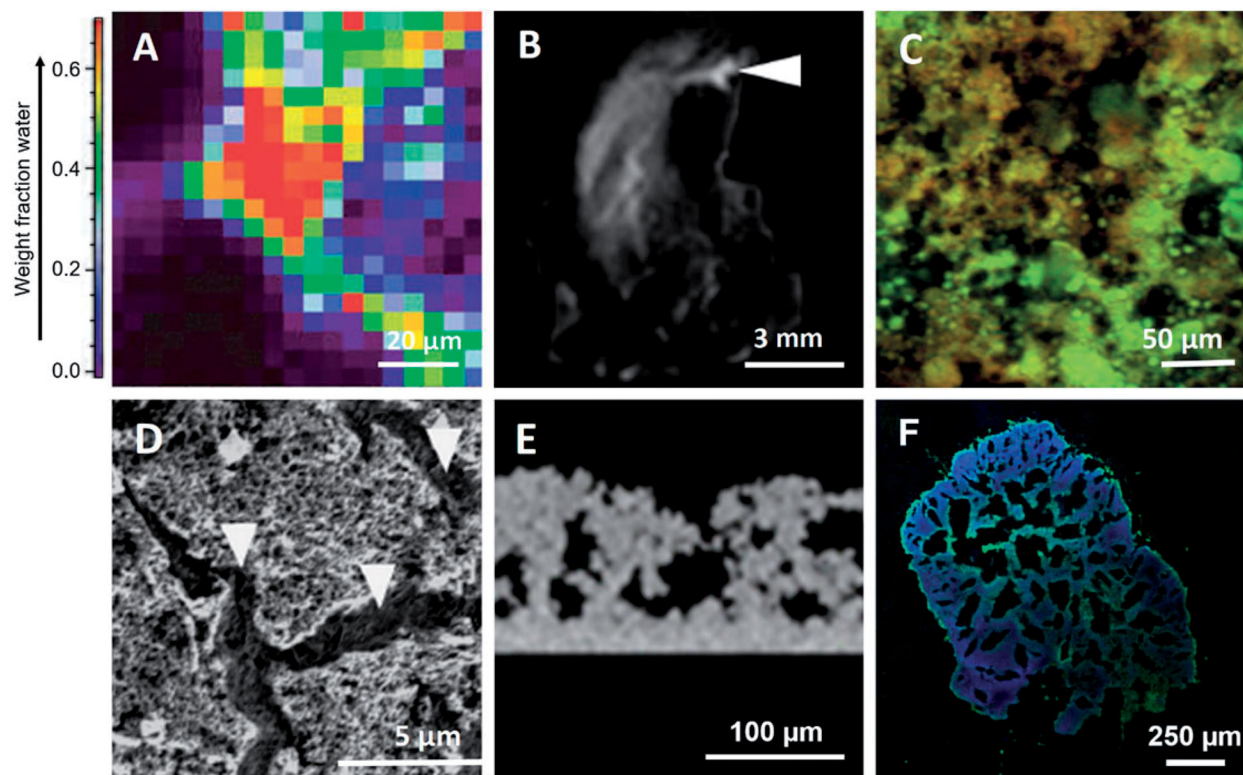


Figure 1. Demonstration of water and visualisation of water-filled regions in biofilms by different techniques. (A) Water-filled region in a *P. aeruginosa* biofilm on stainless steel substratum, affirmatively demonstrated using Raman Micro-spectroscopy (RM) (Sandt et al. 2007). Colour bar indicates the weight fraction of water, ranging from 0 (no water) to 1 (pure water). Reproduced with permission of the publisher, Wiley & Sons Inc. (B) T_2 weighted, Magnetic Resonance Image (MRI) of a natural phototrophic biofilm (Phoenix and Holmes 2008) with affirmative water demonstration. Arrow indicates a water-filled region. Reproduced with permission of the publisher, American Society for Microbiology. (C) Regions in a stained *Streptococcus mutans* biofilm on a dentine surface lacking bacterial fluorescence, assumed to be water-filled, as visualised using Confocal Laser Scanning Microscopy (CLSM) (Galbiatti de Carvalho et al. 2012). Reproduced with permission of the publisher, Faculdade de Medicina da Universidade de Sao Paulo. (D) Regions in a *Vibrio cholerae* biofilm on a stainless steel substratum, assumingly water-filled as visualised using Environmental Scanning Electron Microscopy (ESEM) (Fernández-Delgado et al. 2016). Arrows indicate water-filled regions. Reproduced with permission of the publisher, Instituto de Medicina Tropical de Sao Paulo. (E) Regions in a *S. mutans* biofilm on a polystyrene substratum, visualised using Optical Coherence Tomography (OCT) in which dark areas in the biofilm image are assumed to represent water-filled regions (Wang et al. 2019). Reproduced with permission of the publisher, American Society for Microbiology. (F) Regions in a 15 μm thick slice of an aerobic granular-sludge biofilm devoid of bacterial cells and proteins (as concluded from absence of fluorescence staining), visualised using CLSM and to be water-filled (Courtesy of Maria F. Nava-Ocampo, Andreia S. F. Farinha, Szilárd S. Bucsi, Johannes S. Vrouwenvelder, KAUST, Saudi-Arabia).

Optical coherence tomography (OCT) can also be done non-destructively on hydrated biofilms, and is based on back-scattering of light by particulate matter, such as bacteria or insoluble EPS in a biofilm. Accordingly upon application of an artificial whiteness scale, bacteria in a biofilm appear white in OCT images but the limited resolution of OCT (around 5–10 μm) does not allow imaging of individual bacteria (Haisch and Niessner 2007). Black regions in OCT images have accordingly been interpreted as water-filled regions (Hou et al. 2019), which is likely correct but lacking affirmative confirmation. Changes in signal intensity from black regions in OCT images of biofilms prior to, during and after biofilm compression have been taken as an indication of out- and inflow of water (Hou et al.

2018), providing support for the assumption that these regions were water-filled. Also, average whiteness of biofilm in OCT images has been demonstrated to increase with increasing volumetric bacterial density in biofilms (Hou et al. 2019). Collectively, although these techniques provide evidence of open structures within biofilms that are not filled with bacteria or EPS, that are likely filled with water.

Affirmative evidence and quantification of water in biofilms

Techniques to provide affirmative evidence and quantification of water in biofilms are scarce (Table 1). Dry weight measurements critically depend on a

Table 2. Summary of different techniques to visualise and quantify water in biofilms, together with their advantages and disadvantages, distinguishing between techniques that provide affirmative evidence of water-filled regions in biofilms or only visualise open structures that are generally assumed to be water-filled.

Technique	Advantage and disadvantages	References
Demonstration and quantification of water		
Dry weight measurement	<i>Advantages</i> Yields weight fraction of water in biofilms <i>Disadvantages</i> Not affirmative, destructive, no visualisation, no resolution of structure	(Bratbak and Dundas 1984; Tam et al. 2007)
ATR-FT IR	<i>Advantages</i> Affirmative, distinguishing bound and free water, non-destructive, allowing real-time monitoring, little time-consuming <i>Disadvantages</i> Substrata need to be IR transparent, depth of information restricted to several μm 's, no weight or volume fraction of water content acquired	(Feng et al. 2016; Hou et al. 2018)
RM	<i>Advantages</i> Affirmative, non-destructive, high resolution mapping based on water signals, better detection depth than ATR-FTIR, yields weight fraction of water in biofilms <i>Disadvantages</i> Time consuming, weak water signals, relatively inaccurate compared to dry weight measurement	(Sandt et al. 2007, 2008, 2009; Ivleva et al. 2017)
Visualisation of water-filled regions		
NMR	<i>Advantages</i> Affirmative, distinguishing bound and free water, non-destructive, <i>in situ</i> and real-time monitoring, imaging directly based on water signals, yields volume fraction of extracellular water in biofilms <i>Disadvantages</i> Low spatial resolution, low sensitivity and low signal-noise ratio without assist of paramagnetic reagents	(Seymour et al. 2004; Phoenix and Holmes 2008; Wagner et al 2010)
Light source-based microscopy	<i>Advantages</i> High resolution <i>Disadvantages</i> Not affirmative, particle tracking or fluorescent dyes needed	(Stoodley et al. 1994; De Beer et al. 1997; Galbiatti de Carvalho et al. 2012; Stewart 2012)
ESEM	<i>Advantages</i> High resolution <i>Disadvantages</i> Not affirmative, destructive due to beam damage and reduced pressure	(Bergmans et al. 2005; Fernández-Delgado et al. 2015, 2016)
OCT	<i>Advantages</i> Non-destructive <i>Disadvantages</i> Not affirmative, low resolution not allowing imaging of individual bacteria, image-interpretation not trivial	(Haisch and Niessner 2007)
LLCT	<i>Advantages</i> Yields quantitative data based on visco-elasticities of large volumes of biofilm in one experiment <i>Disadvantages</i> Not affirmative, destructive, no imaging possible, water presence indirectly derived from the time-dependent stress relaxation of compressed biofilms	(Peterson et al. 2013; He et al. 2014; Peterson et al. 2015)

ATR-FT IR: Attenuated total reflection-Fourier transform infra-red spectroscopy; RM: Raman micro-spectroscopy; NMR: nuclear magnetic resonance; ESEM: environmental scanning electron microscopy; OCT: optical coherence tomography; LLCT: low load compression testing.

comparison of a biofilm's weight prior to and after the assumed, complete removal of water by drying, which should be done without affecting the substratum material to which the biofilm adheres (Wilson et al.

2017). However, dry mass measurements are always destructive to the biofilm and do not yield visualisation of the structural biofilm features in which water is confined. Moreover, the concentration of counter ions in

Table 3. Observation timeframes for different techniques to distinguish between free and bound water and binding phenomena and relevance of bound and free water in biofilm.

Timeframe	Observation method	Binding phenomenon	Relevance in biofilms	References
Pico-seconds	ATR-FTIR, RM	Double hydrogen bonding($\cdots\text{H}-\text{O}-\text{H}\cdots$)	- Minor influence on diffusion of water	(Belosludov et al. 2020)
Micro-seconds	NMR lineshape	Reduced rotational diffusion by binding to surfaces, including EPS	- Additional permeation barrier on membranes - Reduced diffusion of nutrients and metabolites - Impact on adhesion	(Vogt et al. 2000)
Milli-seconds	PFG-NMR ^a diffusion measurement	Reduced translational diffusion by encapsulation in <ul style="list-style-type: none"> • pores • channels • membranes (intracellular water) 	- Formation of different water-filled structures	(Vogt et al. 2000)

^aPulsed field gradient NMR.

biofilms will strongly increase with the loss of water, thereby drastically decreasing the chemical potential of the residual water and hampering further drying. Furthermore, it is unclear whether drying removes only “free” water or also “bound” water. Note that the expression “bound” water should not be mistaken for intra-cellularly “confined” water or water “confined” within biofilm (matrix) structures. Bound and free water both have different Infra-red and Nuclear Magnetic Resonance signatures (see also Table 2), that can be used to distinguish between both types of water.

ATR-FT Infra-red (Feng et al. 2016; Hou et al. 2018) spectroscopy affirmatively demonstrates water in biofilms, while also able to differentiate between bound (Van Oss and Giese 2005) and free water. Distinction between bound and free water using ATR-FT Infra-red spectroscopy is relatively easy due to the pico-seconds timeframe required for observation (Table 3) and can be achieved by decomposing the O–H stretching band. A bound water molecule has both hydrogens interacting with a hydroxyl-group (Figure 2), yielding O–H stretching at lower wavelengths ($3250\text{--}3320\text{ cm}^{-1}$) than in free water (O–H stretching at $3320\text{--}3450\text{ cm}^{-1}$). However, ATR-FT Infra-red data only pertain to one or two bacterial layers due to the limited depth of penetration of the evanescent wave into biofilms ($1\text{--}2\text{ }\mu\text{m}$) adhering on ATR crystals employed in FT Infra-red spectroscopy, while moreover without a calibration curve changes in absorption band areas do not yield weight fractions of water, as summarised in Table 1. Raman Micro-spectroscopy is another Infra-red-based technique but has a higher penetration depth than ATR-FT Infra-red up to maximally $200\text{ }\mu\text{m}$ in a biofilm depending on the type of laser used (Sandt et al. 2009), yielding a spatial resolution of $0.5\text{ }\mu\text{m}$ or more. Raman Micro-spectroscopy can generate a micrometer-scale resolution mapping of water presence in biofilms

(Figure 1(A)), as well as of other biofilm components, such as carbohydrates, proteins, lipids and nucleic acids (Sandt et al. 2007). However, Raman Micro-spectroscopy yields relatively weak water signals compared to Infra-red spectroscopy (Ivleva et al. 2017). Water in biofilms has been quantified using confocal Raman Micro-spectroscopy by taking the ratio between the water absorption band around 3450 cm^{-1} and CH_3 absorption band at 2950 cm^{-1} , considered indicative of biomass (Sandt et al. 2008). The quantification of water and biomass in the biofilm was determined with calibration curves from protein solutions. In the upper layers of *P. aeruginosa* biofilms, water represented 92% of the biomass, while in deeper layers of the biofilm water content went down to 88% (Sandt et al. 2008).

Nuclear Magnetic Resonance (NMR) based techniques also affirmatively demonstrate water presence by detecting the proton spin disturbance in a magnetic field. NMR imaging of water in biofilms is based on a micro-second timeframe comparison of the mobility of free water molecules with the mobility of confined or bound water (see also Table 3). Accordingly, bound water will appear as a separate signal in the NMR spectrum due to its reduced rotational mobility. Pulsed field gradient ^1H NMR detected three groups of ^1H NMR signals in *P. aeruginosa* biofilms that were attributed to diffusion of water, that ranged from 2.5×10^{-10} to $1.8 \times 10^{-9}\text{ m}^2\text{ s}^{-1}$. The highest diffusion coefficient was attributed to free water.

Relevance of bound versus free water in biofilms

In physical chemistry, water molecules are said to be bound, when simultaneous hydrogen bonds occur at both hydrogens (Luzar and Chandler 1996). Such hydrogen bonds can occur in water adsorbed to a surface or in free water as temporary clusters (see Figure 2). Unbound water appears as a homogeneous structure

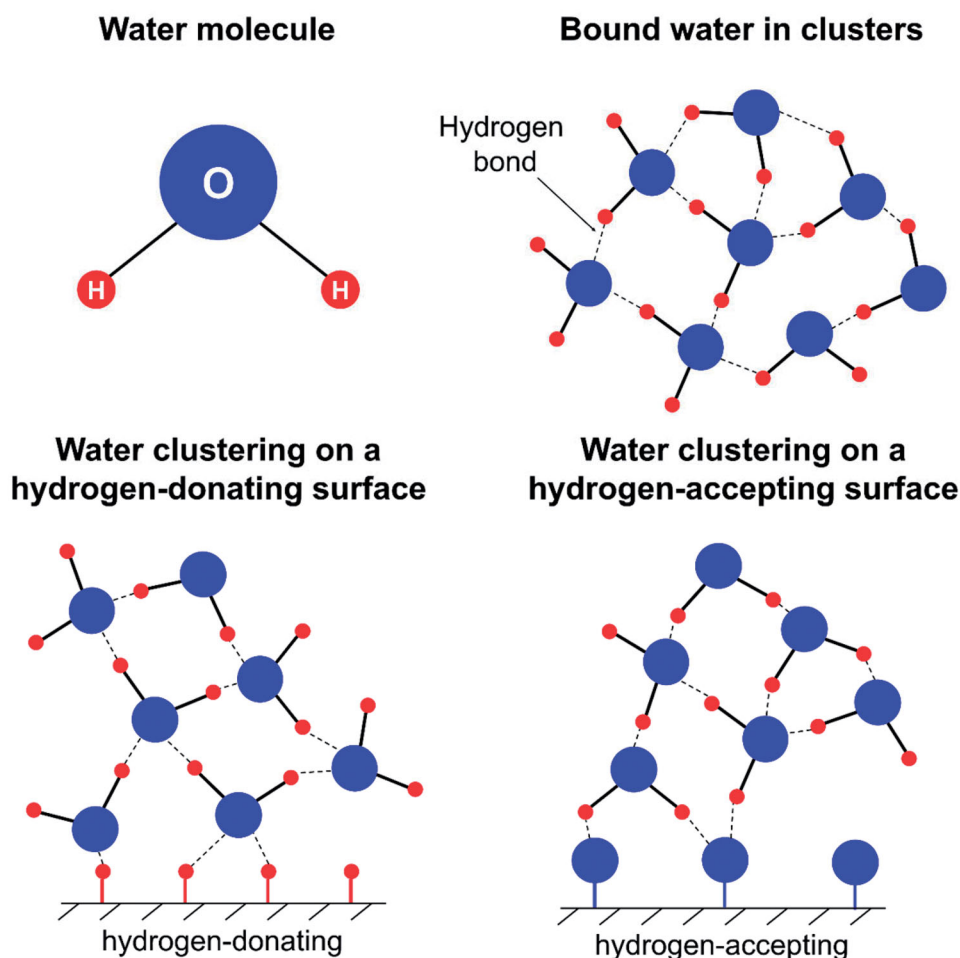


Figure 2. Water adsorbed to a surface consist of a layer of structured water. Structuring ranges up to 1 nm (van Oss and Giese 2005; Björneholm et al. 2016) and depends on the hydrogen-donating and hydrogen-accepting chemical groups on the surface involved.

(Belosludov et al 2020), but actually is a mixture of free, single water molecules and a large multitude of short-lived, “picoseconds” clusters of bound water containing up to 15–20 water molecules. Thus, observation of “bound” or “free” water will depend on the timeframe of observation. As a consequence, depending on the timeframe of the observation method, the transition from bound to free water represents a spectrum of different types of water that can be ranked by the length of time during which water molecules are bound. Different types of water, have different relevance in biofilms (see Table 3). Water in water-filled regions can behave either as free, confined or bound water depending on the dimensions of the water-filled region, affecting convective-diffusion of nutrients and metabolic waste products. The first layer of water bound to a surface can adsorb by acid-base interactions of its hydrogen or oxygen atoms with the surface, depending on whether the surface is composed of hydrogen-donating and hydrogen-accepting chemical groups (Figure 2). The orientation of the second layer of bound

water is determined by whether adsorbed water molecules in the first adsorbed layer are interacting with a surface through their hydrogen or oxygen atoms. The degree of structuring depends on the hydrogen-donating and accepting properties of the surface (see also Figure 2) and decays after a layer thickness of around 1 nm, which corresponds with the size of small clusters of up to 5 water molecules in unbound water (Van Oss and Giese 2005; Björneholm et al. 2016). Therewith, the acid-base character of the underlying surface determines the properties of the outermost surface of a bound water layer, directing the conformation of adsorbed proteins (Zhang et al. 2020) and governing adhesion of bacteria (Zhang et al. 2019; Cai et al. 2021). The structure of water on hydrogen-donating and hydrogen-accepting surfaces depicted in Figure 2 excludes the role of ions. It can be easily envisaged how positively- or negative-charged ions can integrate themselves into a layer of bound water to alter its structure. Accordingly, structuring of bound water decreases with ionic strength (Rehl and Gibbs 2021).

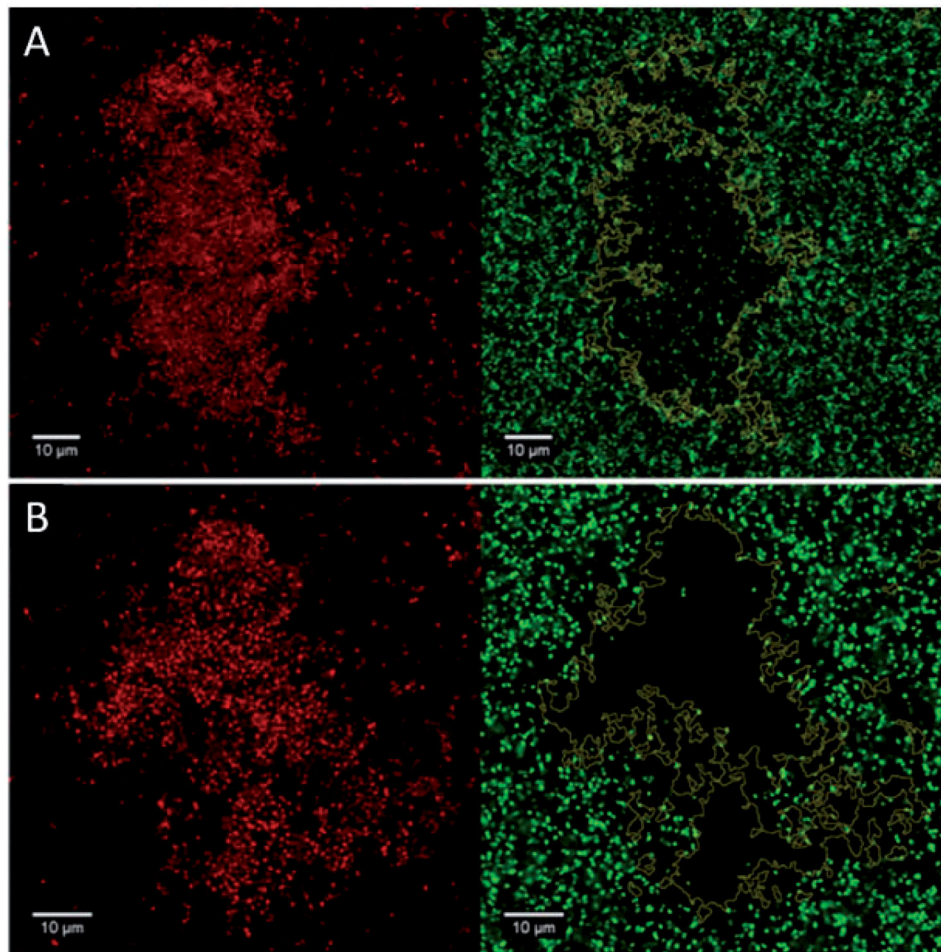


Figure 3. *B. multivorans* biofilms with SYTO 59 stained, red-fluorescent bacterial clusters (left panels) and diffusion-controlled penetration of green-fluorescent poly(ethylene glycol)-coated polystyrene nanoparticles of different diameter (right panels). Note that due to the poly(ethylene glycol)-coating, nanoparticles are unable to adsorb to biofilm components. (A) Particle diameter 129 nm. Green-fluorescent nanoparticles are visible in the biofilm, demonstrating their ability to pass through bacterial clusters. (B) Particle diameter 555 nm (Forier et al. 2014). These larger green-fluorescent nanoparticles are unable to pass through the bacterial cluster surrounding. Reproduced with permission of the publisher, Elsevier B.V.

Structure of water-filled regions in biofilms: channels and pores

Water-filled regions in biofilms exist in between bacterial clusters and within bacterial clusters, that may be held together by EPS or co-adhesion between bacteria in the cluster (Foster and Kolenbrander 2004; Flemming and Wingender 2010). Water-filled structures in a biofilm are often described as channels or pores, without making a proper distinction. Channels and pores are both of vital importance for life in a biofilm. However, it is important to differentiate channels and pores in a biofilm matrix and in this section we propose to distinguish channels and pores based on dimension and function. Channels are by definition long and relatively narrow, connecting two places to facilitate transport and in line, have been called “rudimentary circulation systems in biofilms” (Costerton et al. 1995; Stoodley

et al. 2000). Pores can be distinguished by relatively large volumes without an obvious goal to connect different places, but rather serve as storage and buffering pools (Flemming and Wingender 2010). One rational way to differentiate channels and pores could thus be by using their length/width ratio, although microscopic images from which the length and width of water-filled regions can be measured are scarce.

Transport possibilities through a channel depend on the size of the molecule or particle to be transported, the width of the channel and whether the cargo adsorbs to the channel walls. For example, water-filled regions within bacterial clusters allowed diffusion of an organic dye, such as fluoresceine (MW = 332 Da) or TRITC-IgG (MW = 150 kDa) with diffusion coefficients close to their theoretical values in water. Diffusion of phycoerythrin (MW = 240 kDa) was impeded by 59%

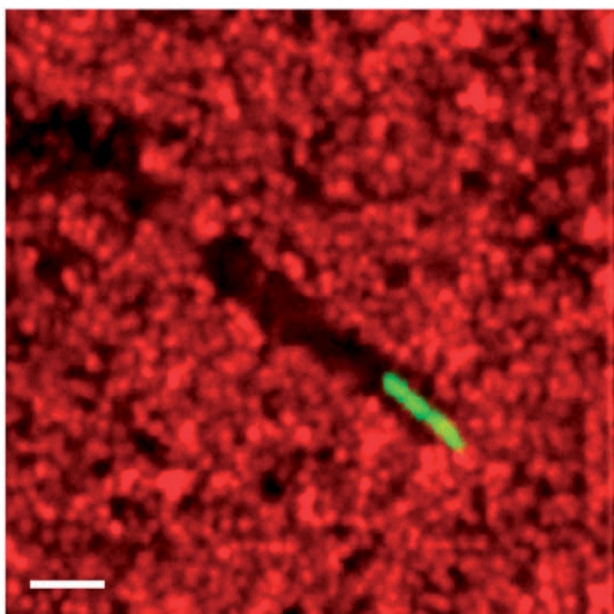


Figure 4. A green-fluorescent GFP *B. thuringiensis* 407 cell added to a red-fluorescent *S. aureus* biofilm creating transient channels in the biofilm matrix (Piard et al. 2017). Scale bar represent 5 μm . Adapted and reprinted with permission of the publisher, IWA Publishing.

relative to water due to adsorption, from which a minimal width of 80 nm for effective diffusion of phycoerythrin was calculated (De Beer et al. 1997), based on the range of interaction forces facilitating adsorption (Van Oss and Giese 2005). Experiments with stealth, poly(ethylene glycol) coated liposomes and polystyrene nanoparticles (see Figure 3), unable to adsorb to biofilm components, demonstrated that liposomes with diameters above 100–130 nm were unable to diffuse through channels in *Burkholderia multivorans* and *P. aeruginosa* biofilms (see Figure 3) (Forier et al. 2014). A similar minimal width of 100 nm was reported in order to avoid adsorption of antimicrobials to channel walls upon diffusion-controlled penetration of an antimicrobial in an infectious biofilm (Ju et al. 2020). However, intra-colony channels with much larger diameters of around 10 μm have also been described in *E. coli*, using giant objective lens microscopy with a high numerical aperture at low magnification (“mesoscopy”) (Rooney et al. 2020) and even wider channels (18–99 μm) have been described in *P. aeruginosa* (Lei et al. 2020). Collectively, it can thus be concluded that biofilm channels effective for transport processes must have a minimal width of around 100 nm.

Besides a minimal width, a water channel should also possess a minimal length in order to achieve effective transport that should at least cover the diameter of an individual bacterium in a biofilm. This yields the suggestion to define a minimal length of at least

1 μm before a water-filled region should be called a channel. This corresponds with visualised channel lengths in *V. cholerae* (Fernández-Delgado et al. 2016), *S. mutans* (Galbiatti de Carvalho et al. 2012), *B. subtilis* (Wilking et al. 2013) and phototrophic (Phoenix and Holmes 2008) biofilms and three species biofilms of *P. aeruginosa*, *Pseudomonas fluorescens* and *Klebsiella pneumoniae* biofilm (De Beer and Stoodley 1995; Stewart 2012). In biofilms of *P. aeruginosa*, channels have been described with a length of around 700 μm , bridging the distance between two places in a biofilm, but these channels had an extremely wide range of widths (Lei et al. 2020). Accepting a minimal length of 1 μm and a width of 100 nm as a characteristic of a channel, channels can be distinguished from pores by a length/width ratio > 10 , while pores should have a length to width ratio closer to one. From published 2D images, it can be roughly derived that on average, pores in *S. mutans* (Galbiatti de Carvalho et al. 2012) and *P. aeruginosa* (Sandt et al. 2007) biofilms indeed have diameters between 30 and 50 μm , with a length/width ratio approaching one.

Mechanisms of channel and pore formation in biofilms

Biofilm channels and pores represent well-designed structures, self-engineered by biofilm inhabitants. The self-engineered nature of these water-filled regions attests to the importance of water-filled channels and pores for life in a biofilm. Highly motile bacillus swimmers from a generally present, planktonic sub-population are known to build water-filled channels by flagella-propelled movement through a biofilm (Houry et al. 2012). For example, *B. thuringiensis* is able to swim through the biofilm matrix of different bacterial strains forming channels (Figure 4). Authors envisaged swimming as a general mechanism persisting in nature since channel building was observed in strains isolated both from medical and industrial surfaces. However, channel building was only effective when the kinetic energy of the swimmers exceeded the visco-elastic resistance of the biofilm matrix, that differed amongst biofilms of *Staphylococcus aureus*, *Enterococcus faecalis*, *Yersinia enterocolitica*, *P. aeruginosa* and *Listeria monocytogenes*. Channels in *E. coli* biofilms have recently been suggested as an emergent property of bacteria in response of their adhesion to a surface (Rooney et al. 2020).

Pores are also self-engineered but their formation is controlled by entirely different mechanisms than channel formation, supporting the distinction made between channels and pores based on function and

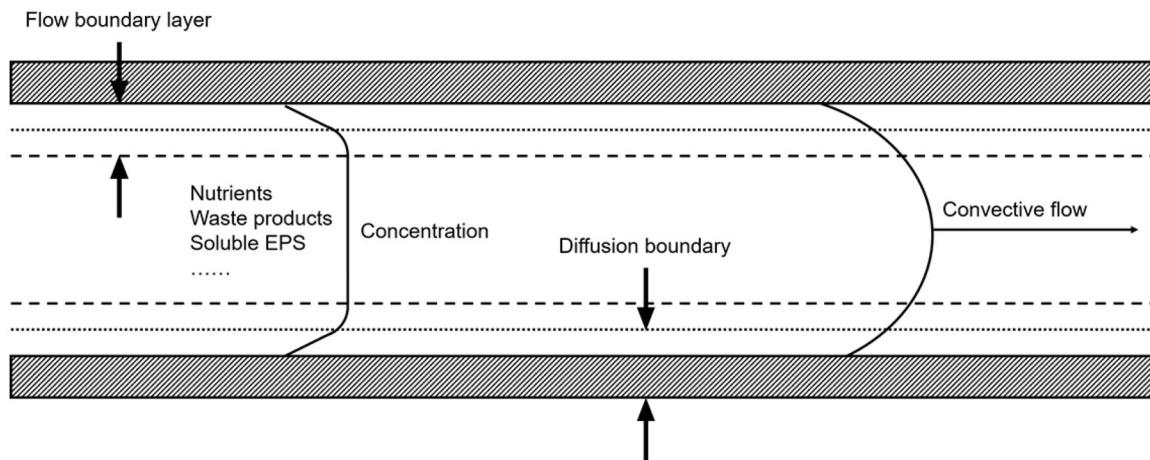


Figure 5. Transport in a channel with convective, Hagen-Poiseuille like flow, driven by a pressure gradient over the length of a channel, prevails in the centre parallel to the channel walls and diffusion is more prominent towards the channel walls, driven by a concentration gradient across the width of the channel.

dimensions. *P. aeruginosa* has been suggested to sacrifice itself in biofilms through lysis to create pores (Webb et al. 2003). More recently, pore formation has been described as a mechanism to reduce the number of biofilm inhabitants in matured EPS biofilms. In a mature biofilm, the inside of a biofilm can locally become fluid giving rise to the development of a planktonic subpopulation in a biofilm and enzymatic weakening of the biofilm matrix (“dispersion”). As a result, the matrix opens up to evacuate the planktonic bacteria and subsequently leaving a central pore in the biofilm (Rumbaugh and Sauer 2020). Therewith dispersion bears similarity with biofilm dispersal, reducing the number of biofilm inhabitants from its interior rather than from the biofilm surface. Dispersion has been described to occur in a large number of different bacterial strains and species (Boles and Horswill 2008; Marks et al. 2013; Piard et al. 2017; Zhou et al. 2017). Dispersion can be induced by environmental as well as internal triggers (Rumbaugh and Sauer 2020).

Channels and pores in biofilms are not necessarily long-lived (Piard et al. 2017) and may collapse or become blocked by visco-elastic expansion of the EPS matrix or bacterial growth, respectively. Biofilm channels and pores are therefore under continuous construction.

Modes of transport in water-filled channels

Water-filled channels in biofilms constitute a crucial means of transport, needed to maintain viability of bacterial inhabitants of a biofilm. Transport in an aqueous phase through channels occurs through convection and diffusion. Convection is driven by a pressure gradient that can either be mechanically or

hydrodynamically applied or arising e.g. from evaporation of water from the surfaces of biofilms (Wilking et al. 2013). Convective mass transport prevails in the length-direction of a channel and is largest in its centre. Diffusion on the other hand, is driven by concentration gradients of the cargo and drives transport towards channel walls through a thin stagnant layer of water bound to the channel wall (the so-called “flow boundary layer,” see Figure 5). Particularly in narrow channels such as in biofilms, adsorption of cargo to the channel walls may occur and hamper transport. In the following two sections, diffusion and convection in biofilms will be described as two separate mass transport mechanisms.

Diffusion in biofilms

In absence of convection, mass transport in bacterial clusters and channels is dependent on diffusion. Effective diffusion coefficients of many molecules (nutrients, waste products and antimicrobials) are several fold lower in biofilms than in water (see Table 4), showing a clear relation with the number of bacteria or biofilm mass per unit biofilm volume (Figure 6). Note that small molecules and ions have effective diffusion coefficients in biofilm that are little smaller than in water. Differences between effective diffusion coefficients and water become much larger when larger molecules are involved due to stronger adsorption to channel walls. Adsorption to channel walls and impact of bound water vary across biofilms of different strains. To this point, the effective diffusion coefficient of high (2000 kDa) molecular dextran is two-fold higher in a mixed species biofilm than in a *P. aeruginosa* biofilm (Table 4), possibly due to a different orientation of

Table 4. Overview of diffusion coefficients of selected molecules in different biofilm and in water.

Transported molecules	Type of biofilm	Effective diffusion coefficient in biofilms ($\text{cm}^2 \text{s}^{-1}$)	Diffusion coefficient in water ($\text{cm}^2 \text{s}^{-1}$)	References
NH_4^+	<i>Nitrobacter</i>	13.9×10^{-6}	17.4×10^{-6}	(Williamson and McCarty 1976)
NO_2^-		13.9×10^{-6}	16.2×10^{-6}	
O_2		25.4×10^{-6}	30.0×10^{-6}	(Stewart et al. 2001)
Cl^-	Mixed species biofilm	$1.4\text{--}1.9 \times 10^{-5}$	2.0×10^{-5}	
Phenol	Mixed species	2.2×10^{-6}	8.5×10^{-6}	
Fluorescein (289 Da)	Mixed species	7.7×10^{-8}	3.3×10^{-6}	(Lawrence et al. 1994)
Dextran (4 kDa)		3.1×10^{-8}	1.5×10^{-6}	
Dextran (40 kDa)		1.7×10^{-8}	0.7×10^{-6}	
Dextran (2000 kDa)		0.7×10^{-8}	5.6×10^{-8}	
Fluorescein (289 Da)	<i>Pseudomonas fluorescens</i>	1.0×10^{-8}	3.3×10^{-6}	(Lawrence et al. 1994)
Dextran (2000 kDa)		0.3×10^{-8}	5.6×10^{-8}	
Chlorhexidine	<i>Candida albicans</i>	$3.2\text{--}8.9 \times 10^{-7}$	31×10^{-7}	(Suci et al. 2001)
Rhodamine B (442 Da)	<i>S. epidermidis</i>	$0.2\text{--}0.7 \times 10^{-6}$	3.6×10^{-6}	(Rani et al. 2005)
Fluorescein (376 Da)	<i>S. epidermidis</i>	$1.0\text{--}2.1 \times 10^{-6}$	4.9×10^{-6}	
Ciprofloxacin (330 Da)	<i>P. aeruginosa</i>	$1.5\text{--}9.0 \times 10^{-10}$	33.4×10^{-8}	(Suci et al. 1994)
Tobramycin (468 Da)	<i>P. aeruginosa</i>	0.9×10^{-8}	15.3×10^{-8}	(Sankaran et al. 2019)
Ciprofloxacin (330 Da)		1.3×10^{-8}	33.4×10^{-8}	
Dextran (2000 kDa)		6.0×10^{-8}	15.9×10^{-8}	

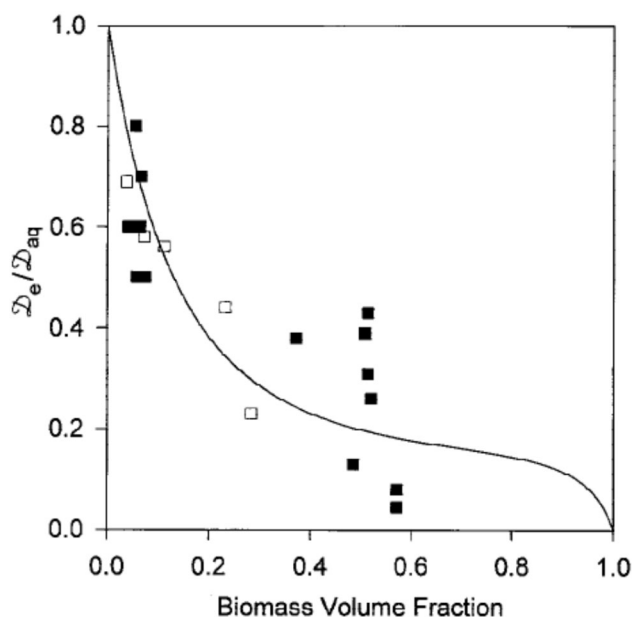


Figure 6. Diffusion coefficients D_e of large (closed symbols) and small solutes (open symbols) as a function of the volume fraction of biomass in biofilms expressed relative to their diffusion coefficient D_{aq} in water (Stewart 1998). Reproduced with permission of the publisher, Wiley & Sons, Inc.

water molecules bound to channels in the matrix of both biofilms. Due to the structural and compositional heterogeneity in many biofilms, such as gas bubbles, precipitates, and locally changing biofilm densities in deeper (Herrling et al. 2017) or more shallow regions of a biofilm (Renslow et al. 2010), effective diffusion

coefficients in biofilms often do not have a single value but present a broad distribution. Pulsed field gradient-Nuclear Magnetic Resonance demonstrated that a small molecule like water, shows three fractions with different diffusion coefficients in *P. aeruginosa* biofilms (Vogt et al. 2000). Free water was identified as possessing the highest diffusion coefficient. Two other fractions had much lower diffusion coefficients probably arising from confined water and diffusion of water in through water-filled channels in bacterial clusters. Thus effective molecular diffusion coefficients in water-filled channels may be much lower than of free and confined water, particularly in bacterial clusters (Wood et al. 2002; Stewart 2003). Occurrence of broad distributions of effective diffusion coefficients can be expected to be even larger in multi-species biofilms than in single-species biofilms (Herrling et al. 2017).

Convection in absence and presence of applied pressures on a biofilm

In absence of applied pressure, convective mass transport through biofilm channels is low. Often, however, biofilms grow while exposed to convective flow that can extend into near-surface structures of a biofilm, gaining access to a biofilm through channels in mushroom-shaped and other irregular surface morphologies. Transport from deeper layers of a biofilm subsequently relies predominantly on diffusion. Also, upon application of an external pressure such as in membrane

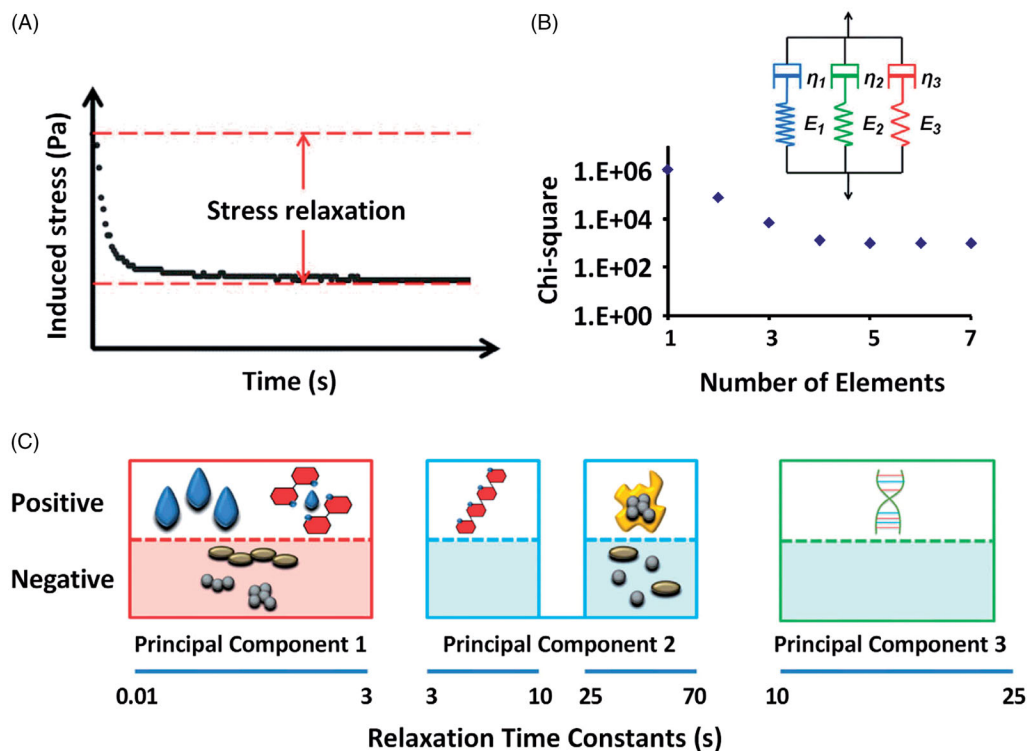


Figure 7. Stress relaxation and water flow during low load compression of biofilms and Maxwell analyses. (A) Example of the normalised stress exerted by a compressed biofilm as a function of relaxation time. Stress was applied at $t = 0$ (He et al. 2013). (B) A three component generalised Maxwell model, in which each element possesses its own characteristic relaxation time, usually suffices to describe stress relaxation in biofilms. One Maxwell element is composed of a spring and a dashpot, representing an elastic and a viscous response, respectively (He et al. 2013; Peterson et al. 2013). Reproduced with permission of the publisher, American Society for Microbiology. (C) Principal components in stress relaxation of biofilms with the relaxation time constant range < 3 s associated with in- and outflow of water in absence and presence of soluble polysaccharides, insoluble polysaccharides (3–10 s and 25–70 s) and presence of eDNA (10–25 s) (Peterson et al. 2013). Reproduced with permission of the publisher, American Society for Microbiology.

filtration, convective fluid flow can develop in biofilms. Flow velocities developing in biofilms differ between the small channels in bacterial clusters and wider channels within the EPS matrix, depending on the hydraulic resistance (Dreszer et al. 2013) of the channels.

Stoodley et al. (1994) tracked the movement of 0.3 μm diameter fluorescent beads using CLSM in a mixed-species biofilm grown in a porous medium reactor. Upon application of a hydrodynamic pressure, a water flow velocity in channels of around 10–20 $\mu\text{m}/\text{s}$ was measured, similar as in *B. subtilis* biofilms (Wilking et al. 2013). However, the 0.3 μm diameter fluorescent beads were unable to penetrate into a bacterial cluster indicative of smaller channels in bacterial clusters than in the biofilm as a whole. Also, other studies using time-lapse CLSM (Rani et al. 2005; Stewart et al. 2009) or Nuclear Magnetic Resonance (Hornemann et al. 2009; Wagner et al. 2010) of biofilms under hydrodynamic pressure (Stewart 2012), suggested the absence of convection inside bacterial clusters (Stewart 2012).

Upon application and relaxation of low mechanical pressures, convective water in- and outflow during compression of biofilms through biofilm channels can be observed (Peterson et al. 2014; Hou et al. 2018). Under low load compression, a biofilm is compressed typically to less than 50% deformation, after which the resulting decrease in stress is monitored as a function of time (see Figure 7(A)). Subsequently, stress relaxation over time is fitted by a three component Maxwell model (Figure 7(B)), yielding the relative importance of each Maxwell element and their relaxation time constants (Peterson et al. 2013; He et al. 2014; Peterson et al. 2015). The relaxation time constant in a Maxwell element is modelled by a spring, representing an immediate response and a dashpot in parallel with the spring, slowing down the immediate response. In general, relaxation of a biofilm from an applied mechanical stress is described by three Maxwell elements. The Maxwell elements with slower relaxation times have been associated with convection of more viscous (possibly water-dissolved) EPS components and re-

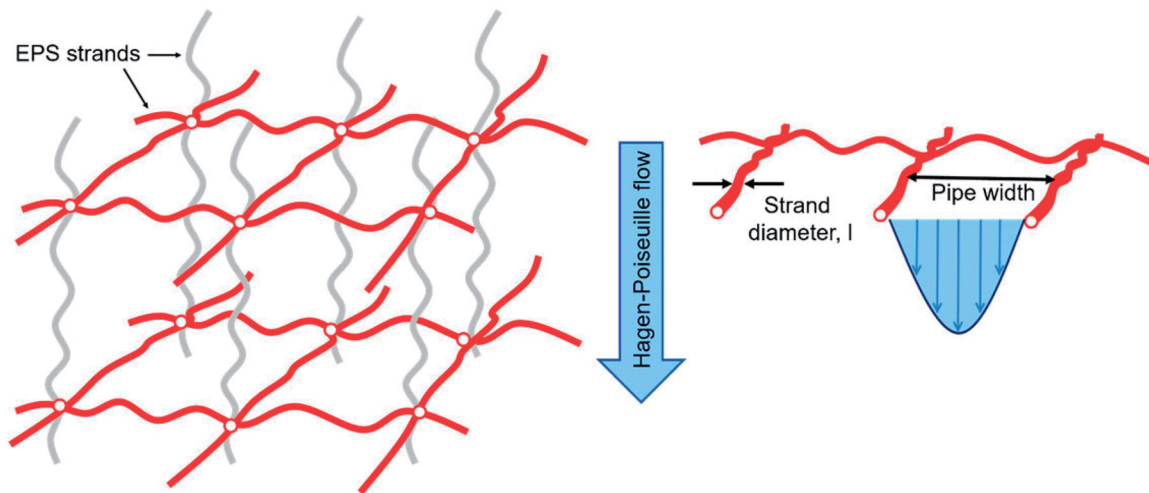


Figure 8. Schematic representation of the gel-like EPS matrix structure as existing in a compressed biofilm after exposure to pressure. The matrix can be envisaged as a rectangular network of EPS strands and in each single mesh, a Hagen–Poiseuille flow will develop (Vrouwenvelder et al. 2017). Adapted and reprinted with permission of the publisher, IWA publishing.

positioning of bacteria within a compressed biofilm (Figure 7(C)). Biochemical analyses have confirmed the association with EPS components (Peterson et al. 2013), while microscopy has confirmed bacterial re-arrangement (Peterson et al. 2014). The fastest relaxation is assumed to be associated with free water presence in a biofilm, as water possesses the lowest viscosity in a biofilm and most easily forced to flow through a channel. The relative importance of the Maxwell component associated with convective flow of water increased when the compression of a biofilm increased, although water itself is principally incompressible. This demonstrates that water flow plays an important role in the recovery of a deformed biofilm towards its natural state, although full recovery of a mechanically deformed biofilm to its initial state seldom occurs (Jafari et al. 2018; Oyebamiji et al. 2018). Visco-elastic properties of biofilms are not homogeneously distributed over a biofilm and mushroom-shaped microcolonies in *P. aeruginosa* biofilms, for instance, were softer than plain biofilm regions (Kundukad et al. 2016), due to more extensive EPS expression in microcolonies.

Biofilm channels under compression

Depending on the pressure applied, channels and pores will be compressed (Kundukad et al. 2016), leading to the formation of a dense gel-like matrix of bacteria and EPS (Figure 8). The compressed EPS matrix can be represented as a three-dimensional molecular network of EPS strands. Water flow through the meshes of the EPS strands in a compressed biofilm under pressure, as e.g. in oral biofilms during mastication or in biofilms on

membrane filters, can be described by the Hagen–Poiseuille approach (see also Figure 8).

The volumetric flow in each of these meshes can be approximated as a flow in a short rectangular “pipe” with an approximate width of 10 nm (Vrouwenvelder et al. 2017) according to

$$v = \frac{Kl^2 \left(\frac{3}{V_{rel}}\right)^{3/2} \Delta P A}{12 \eta d} \quad (1)$$

where the constant K refers to the cross-sectional geometry of the mesh and amounts 0.4218 in case of a rectangular pipe (Bruus 2008), l is the diameter of the EPS strand, ΔP is pressure drop across the EPS gel, A is the total area of the compressed biofilm section considered, d is the thickness of the biofilm considered, V_{rel} is the volume fraction of EPS in the biofilm and is the viscosity of water with or without dissolved EPS components. Equation (1) implies that the volumetric flow at a given pressure drop would scale with $V_{rel}^{-3/2}$. Accordingly, an increase of the EPS content in a biofilm by a factor of four due to compression under pressure, would lead to a decrease of the volume flow of water by a factor of eight which may severely impact vital transport processes in the biofilm. Alternatively, Equation (1) also allows to predict the effect of biofilm compression on volumetric flow within a biofilm. Scaling the biofilm thickness d by a factor of x , reflecting its compression, leads to a corresponding change of the EPS volume fraction by a factor of $1/x$. If both variations enter Equation (1), this results in a total variation of the volumetric flow by a factor of $x^{1/2}$. Accordingly, if the biofilm is compressed to one fourth

of its original thickness, volumetric flow decreases by a factor of two.

Experimental verification of the EPS gel structure model has proven it to be reliable. In membrane filtration, the model showed that the resistance of a biofilm under pressure against compression is largely due to the EPS matrix and not to the bacterial cells in the biofilm (Dreszer et al. 2013; Vrouwenvelder et al. 2017). Interestingly, also the visco-elastic relaxation of bacterial biofilms after pressure (see Figure 7(A)) depended critically on the presence of an EPS matrix. Rearrangement of bacteria in a compressed biofilm after pressure relieve could only be observed in biofilms of an EPS producing *P. aeruginosa* strain but not in an isogenic mutant deficient in production of EPS (Peterson et al. 2014). In an *S. aureus* biofilm, production of polysaccharides per bacterium in the initial layer of adhering staphylococci was higher during growth at high shear than at low shear and this increased EPS production extended to entire biofilms. Compression of staphylococcal biofilms grown under high fluid shear yielded an immediate increase in FT Infra-red polysaccharide absorption band area that decreased after relieving pressure to the level observed prior to compression due to outflow and inflow of water, respectively (Hou et al. 2018). Thus, EPS functions to resist biofilm compression under pressure and also aids to re-open channels in pores therewith safeguarding transport through a biofilm.

Osmosis as a driving force for water flow in a biofilm

Osmotic pressure differences in relation with the flow of water in biofilms has not yet been frequently studied. Biofilms can exist both at low (water) and high osmotic pressure (high salt concentration, as in seawater). The osmotic pressure in a biofilm is maintained by the matrix and provides an important regulator in the response of a biofilm to different environments, facilitating expansion or relaxation of a biofilm by in- and out-flow of water (Seminara 2012). This type of expansion is promoted by growing bacteria creating the required osmotic pressure difference when on a nutrient-rich surface facilitating nutrient uptake (Yan et al. 2017). Although described for *Vibrio cholerae*, it is suggested to be general in different bacterial strains and species.

The roles of water-filled channels and pores in biofilms

Water-filled channels and pores in biofilms have been suggested to be part of a so-called “rudimentary

vascular system,” performing similar roles as the human vascular system (Houry et al. 2012; Gerbersdorf and Wieprecht 2015). In this section, we present examples of the roles that water-filled channels and pores play in diverse, selected biofilms justifying the expression “rudimentary vascular system,” including options to create artificial, additional channels as by-passes in the rudimentary vascular system of infectious biofilms.

Transport and storage of nutrients and waste products

Transport of nutrients and waste-products is of vital importance for biofilm life. Biofilm formation starts with the adhesion of single bacteria, often from a flowing, nutrient-containing fluid. This implies ample nutrient availability that reduces upon growth to a multi-layered biofilm. Without specific structural features, nutrients would not be available throughout an entire biofilm which requires a smart design of the biofilm matrix. Particularly channels in high-density clusters in biofilms have been identified as functional for nutrient transport and acquisition (Rooney et al. 2020), utilising osmotically driven biofilm expansion as a driving force for water flow (Yan et al. 2017). Bacteria residing in deeper layers of a biofilm usually receive less nutrients due to the long distance from the biofilm surface that needs to be bridged by channels and consumption of nutrients on the way to the bottom (Seymour et al. 2004; Wilking et al. 2013). This is evidenced by the observation that the percentage viable bacteria decreases deeper inside a biofilm, as demonstrated in biofilms of *Staphylococcus aureus* Xen29, *S. aureus* Xen36, *E. coli* Xen14, *P. aeruginosa* PA14 and CNS (coagulase negative staphylococcus) DN7334 (Sjollema et al. 2011). In order to compensate as much as possible for periods of nutrient deprivation, water-filled pores serve for nutrient storage to feed bacteria deeply located in biofilm clusters (Houry et al. 2012). In *Pseudomonas syringae* biofilms, accumulation of nutrients (levan) in storage pores has been observed using CLSM (Laue et al. 2006). As a last resort solution, when channels do not allow sufficient means for nutrient transport and waste storage and pores insufficiently dilute waste-products, dormancy may develop in deeper layers of a biofilm.

Transport and accumulation of auto-inducers

Quorum-sensing (QS) is a mechanism by which bacteria in a biofilm can communicate by diffusion of small molecules to regulate group response (Yang et al. 2010).



Figure 9. A macroscopically visible, curled up “biofilm-skin,” developing in an environmental biofilm on the mortar of a brick wall upon drying. The interaction between the EPS molecules and the sand grains in the mortar can become so strong that during the curling process, grains are pulled out of the mortar (Flemming 2008). Reproduced with permission of the publisher, Springer Int. Berlin, Heidelberg, Germany.

Quorum-sensing is mediated by the excretion of auto-inducers. Auto-inducers are small soluble molecules that are transported in a biofilm through diffusion (Abraham 2016) and when present above a so-called threshold concentration, stimulate response in other bacteria. “Calling” distances over which bacteria can communicate through quorum-sensing have been reported between 4 μm and 78 μm in *P. putida* biofilms, as mediated by N-acylhomoserine lactone (Gantner et al. 2006). Channels as defined in this review, are imperative for quorum-sensing over long distances, as diffusion in dense bacterial clusters is small and auto-inducers accumulate in clusters (Darch et al. 2012). Quorum sensing can be repressed in bacteria close to a biofilm surface exposed to flow, but remained operative near the bottom of a biofilm, where autoinducers remained to be accumulated in high concentrations (Kim et al. 2016). This suggests a role of near-surface channels in making a biofilm accessible to convective fluid flow and diffusion of auto-inducers to deeper layers of a biofilm, while at the same time preventing accumulation of autoinducers above their threshold concentration at more shallow depths.

Evaporation of water from biofilms

One of the driving forces for convective fluid flow in biofilm channels is the evaporation of water (Wilking et al. 2013), that deprives a biofilm of an important means for transport and storage. Upon evaporation, the free water content decreases, as has been concluded from decreases in infrared absorption bands around 3350cm^{-1} , indicative of the loss of free water in *Campylobacter jejuni* biofilms (Feng et al. 2016). After removal of free water, bound water may disappear depending on temperature leading to increased Lifshitz-Van der Waals binding (van Oss 2003) between remaining EPS molecules. Similar as occurring within hydrogels upon drying (Hobley et al. 2013; Decho 2017), this mechanism is responsible for outward curling of a so-called “biofilm-skin” that can be macroscopically observed with the naked eye (Figure 9). The biofilm skin retains the underlying water due to its hydrophobicity and provides another kinetic barrier against further loss of water and counts as one of the natural protection mechanisms offered by the biofilm-mode of growth for its inhabitants to survive dry conditions. Simultaneously with the evaporation of water, the ionic strength in the biofilm will increase which will lead to a lack of electrostatic double-layer stabilisation, that stimulates compression of biofilms (Decho 2017; Decho and Gutierrez 2017). In environments with extremely high salinities, this effect will be strongest and lead to the formation of a hard “plastic-like” biofilm.

Dewatering of sewage sludge

Sewage sludge is highly hydrated and an inevitable by-product of biological wastewater treatment, containing more than 92% water, various solids, and different bacterial strains (Anjum et al. 2016). Sewage sludge needs to be dewatered in order to prepare the sludge for agricultural application, deposition or incineration. Upon dewatering, the sludge is aggregated into flocs, which are then further condensed to a sludge cake (Cao et al. 2016) in which bacteria and solid waste are closely associated in a biofilm-like manner. Filtration or centrifugation removes the water through channels during sludge cake formation, aided by acidic or alkaline pre-treatment, addition of flocculants, chemicals, enzymes, electrochemical, microwave or ultrasonic treatment (Wu et al. 2020; Wei et al. 2018). Such combined treatments remove free water and in part also bound water (Erdincler and Vesilind 2003). Channels collapse at higher filtration or centrifugation pressures which can be prevented by addition of e.g. lime or fly ash (Qi et al.

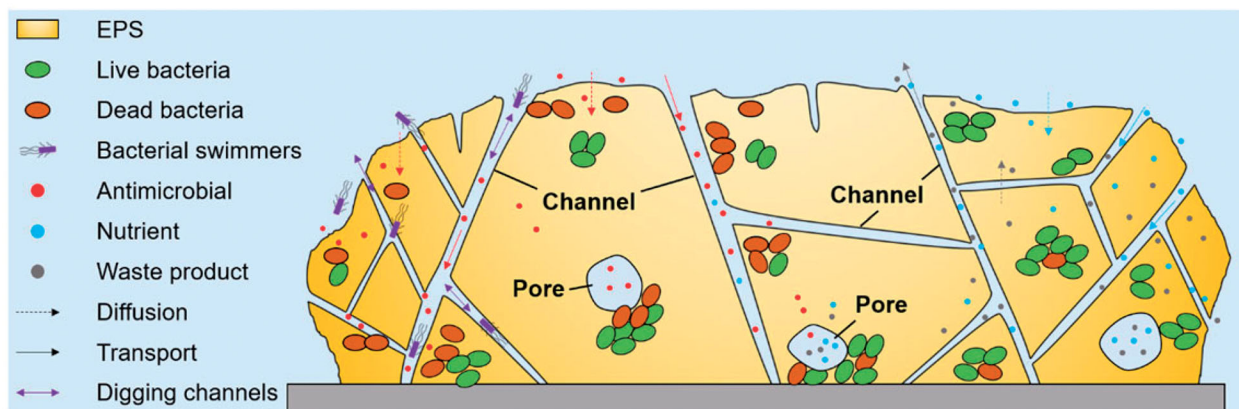


Figure 10. Schematics of water-filled channels and pores in a biofilm as self-engineered by bacterial swimmers, dispersion and lysis, together with their respective transport and storage functions and mass transport mechanisms. Note, channels by its proposed definition always connect two places in a biofilm or allow access to the biofilm, while pores are isolated and confined, without a connection to other places in the biofilm. Artificially created by-passes enhanced transport to allow e.g. deeper penetration of antimicrobials for the control of infectious biofilms or to increase the yield of electroactive biofilms.

2011; Zhu et al. 2012). However, in practical operation this has appeared difficult and current dewatering of sludge must be improved in order to mitigate the high energy demand and costs of sludge dewatering (Xu et al. 2020). A detailed knowledge of water binding in biofilms is crucial for further efforts in this direction.

Antimicrobial penetration and killing: impact of water-filled channels and pores

The efficacy of antimicrobial treatment is known to be hampered by poor penetration of antimicrobials into a biofilm ever since Van Leeuwenhoek (1684) observed that the vinegar with which he washed his teeth killed only bacteria at the outside of a biofilm. Arguably, breaking down the penetration barrier posed by the biofilm-mode of growth of infectious biofilms, might be a more effective way to contain the threat of antimicrobial resistant infections than the development of new antibiotics, that are generally short-lived through the development of new resistance (Liu et al. 2020).

Water plays a dual role in antimicrobial penetration and killing in which particularly the distinction between channels and pores is crucial. Limited antimicrobial penetration into most naturally occurring biofilms is due to lack of sufficiently wide channels (Houry et al. 2012) and antimicrobial adsorption to channel walls in natural biofilms. This impedes the build-up of a high antimicrobial concentration in the depth of a biofilm. Although this would suggest that a biofilm with a higher water content might be more amenable to antimicrobial penetration and killing, this is only true for water-filled channels. Stress relaxation analysis of single-species oral biofilms grown *in vitro* actually demonstrated that the efficacy of chlorhexidine killing

decreased with the importance of the fast relaxation element, representing the ability of water to flow through channels in and out of a biofilm. This conclusion drawn from *in vitro* experiments with single species oral biofilms, could be confirmed in multi-species *ex vivo* oral biofilms (Stewart 2003). A high water content in biofilms due to water-filled pores decreased antimicrobial killing, likely because water-filled pores acted as a buffer pool, diluting the antimicrobial concentration to below its minimal bactericidal concentration (Stewart 2003).

Conclusions and outlook

Techniques to study water-filled regions in biofilms can be separated in two classes of techniques that allow to visualise structures in a biofilm that are subsequently assumed to be water-filled, and techniques that yield affirmative evidence of water presence in such structures. Especially Infra-red- and Nuclear Magnetic Resonance-based techniques have proven useful for affirmative demonstration of water presence and allowed to distinguish free water and water bound to bacterial cell surfaces or the EPS matrix of biofilms, although the differentiation depends on the timeframe of observation. Bound water adds to the barrier function of bacterial membranes and affects the adhesiveness of EPS. Water-filled regions predominantly contain free water and either serve a transport function when their length is much larger than their width (“channels”) or serve to store e.g. nutrients and as a buffer to dilute waste-products or antimicrobials when they possess roughly equal length to width ratios (“pores”). Both channels and pores perform functions that are vital to biofilm inhabitants (Figure 10), which is the reason why

bacteria have the ability to self-engineer channels and pores through swimming, dispersion, lytic self-sacrifice or adaptive responses. Natural, self-engineered channels are often transient and convective fluid flow in absence of an applied pressure on the biofilm is low. Therefore, most transport in biofilms is due to relatively slow diffusion, hampered by cargo adsorption to channel walls.

Based on the insights provided into the formation of biofilm channels and pores, their vital roles in transport and storage within a biofilm, new strategies to enhance the yield of bioreactors or susceptibility of infectious biofilms to antimicrobials can be developed. Non-contact, sonic-brushing of oral biofilms has been demonstrated to affect the visco-elastic properties of biofilm and therewith its structural features to enhance killing by penetrating antimicrobials (He et al. 2014). Inspired by ability of swimming bacteria to create biofilm channels, creation of by-pass channels has been explored as a new antimicrobial strategy to add channels to *S. aureus* biofilms (Figure 4) in addition to naturally occurring channels to make the biofilm more amenable to antibiotic penetration (Houry et al. 2012). As a synthetic analogue, magnetic iron oxide nanoparticles have been moved under an applied, external magnetic field through *S. aureus* biofilms to create additional, artificial channels that enhanced antibiotic penetration and bacterial killing (Quan et al. 2019). The artificial channels created by magnetic nanoparticles were around 100 nm in width, which is much smaller than microbially-engineered channels formed by bacterial swimmers (see Figure 4). By-pass channels artificially engineered using magnetic nanoparticles were stable over a time-scale of at least 1–3 h and less susceptible to visco-elastic collapse probably as a result of their smaller width. Channel formation in biofilms by magnetic nanoparticles as an anti-biofilm strategy to control human infection, is preferable above microbial-engineering of channels, as this would involve adding another bacterial strain to an already infected patient. In electroactive biofilms (Jones and Buie 2019), additional, artificially-engineered channels may increase bacterial metabolism and therewith electric current production. Controlling of the adaptive response of adhering bacteria to influence the structural features of biofilms has not been explored to our knowledge, in absence of solid knowledge of the properties of a substratum surface that control the adaptive response of initial colonisers of a surface (Ren et al. 2018). The adhesion forces experienced from a substratum surface by initially adhering bacteria have been suggested as a candidate trigger for adaptive responses (Carniello et al. 2018) and further

research on the influence of adhesion forces on the formation of channels and pores in biofilms seems warranted.

Disclosure statement

HJB is a director of a consulting company SASA BV. The authors declare no potential conflicts of interest with respect to authorship and/or publication of this article. Opinions and assertions contained herein are those of the authors and are not construed as necessarily representing views of the funding organization or their respective employer(s).

Funding

This study was funded by UMCG, Groningen, The Netherlands, Natural Science Foundation of the Jiangsu Higher Education Institutions of China [20KJA150008], the National Natural Science Foundation of China [21522404].

ORCID

Jiapeng Hou  <http://orcid.org/0000-0002-1025-0842>
 Yijin Ren  <http://orcid.org/0000-0002-2374-1771>
 Henny C. van der Mei  <http://orcid.org/0000-0003-0760-8900>

References

- Abraham W-R. 2016. Going beyond the control of quorum-sensing to combat biofilm infections. *Antibiotics*. 5(1):3.
- Anjum M, Al-Makishah NH, Barakat MA. 2016. Wastewater sludge stabilization using pre-treatment methods. *Process Saf Environ Prot*. 102:615–632.
- Belosludov V, Gets K, Zhdanov R, Malinovsky V, Bozhko Y, Belosludov R, Surovtsev N, Subbotin O, Kawazoe Y. 2020. The nano-structural inhomogeneity of dynamic hydrogen bond network of TIP4P/2005 water. *Sci Rep*. 10(1):7323.
- Bergmans L, Moisiadis P, Van Meerbeek B, Quirynen M, Lambrechts P. 2005. Microscopic observation of bacteria: review highlighting the use of environmental SEM. *Int Endod J*. 38(11):775–788.
- Björneholm O, Hansen MH, Hodgson A, Liu L-M, Limmer DT, Michaelides A, Pedevilla P, Rossmesl J, Shen H, Tocci G, et al. 2016. Water at Interfaces. *Chem Rev*. 116(13): 7698–7726.
- Boles BR, Horswill AR. 2008. Agr-mediated dispersal of *Staphylococcus aureus* biofilms. *PLoS Pathog*. 4(4): e1000052.
- Bratbak G, Dundas I. 1984. Bacterial dry matter content and biomass estimations. *Appl Environ Microbiol*. 48(4): 755–757.
- Bruus H. 2008. *Theoretical microfluidics*. Oxford: Oxford University Press; p. 37–90.
- Byers JD, Drummond F. 1998. Local macromolecule diffusion coefficients in structurally non-uniform bacterial biofilms using fluorescence recovery after photobleaching (FRAP). *Biotechnol Bioeng*. 60(4):462–473.

- Cai L, Chen J, Chang L, Liu S, Peng Y, He N, Li Q, Wang Y. 2021. Adhesion mechanisms and electrochemical applications of microorganisms onto a GO-NH₂ modified carbon felt electrode material. *Ind Eng Chem Res.* 60(11): 4321–4331.
- Cao B, Zhang W, Wang Q, Huang Y, Meng C, Wang D. 2016. Wastewater sludge dewaterability enhancement using hydroxyl aluminum conditioning: role of aluminum speciation. *Water Res.* 105:615–624.
- Carniello V, Peterson BW, Van der Mei HC, Busscher HJ. 2018. Physico-chemistry from initial bacterial adhesion to surface-programmed biofilm growth. *Adv Colloid Interface Sci.* 261:1–14.
- Chan WP, Wang JY. 2016. Comprehensive characterisation of sewage sludge for thermochemical conversion processes – based on Singapore survey. *Waste Manag.* 54:131–142.
- Costerton JW, Lewandowski Z, Caldwell DE, Korber DR, Lappin-Scott HM. 1995. Microbial biofilms. *Annu Rev Microbiol.* 49:711–745.
- Coulibaly I, Dubois-Dauphin R, Destain J, Fauconnier M-L, Lognag G, Thonart P. 2010. The resistance to freeze-drying and to storage was determined as the cellular ability to recover its survival rate and acidification activity. *Int J Microbiol.* 2010:625239.
- Darch SE, West SA, Winzer K, Diggle SP. 2012. Density-dependent fitness benefits in quorum-sensing bacterial populations. *Proc Natl Acad Sci U S A.* 109(21):8259–8263.
- De Beer D, Stoodley P. 1995. Relation between the structure of anaerobic biofilm and transport phenomena. *Water Sci Technol.* 32(8):11–18.
- De Beer D, Stoodley P, Lewandowski Z. 1997. Measurement of local diffusion coefficients in biofilms by microinjection and confocal microscopy. *Biotechnol Bioeng.* 53(2): 151–158.
- Decho AW. 2017. In: Flemming HC, Neu TR, Wingender J, editors. *The perfect slime: microbial extracellular polymeric substances.* London: IWA Press; p. 207–220.
- Decho AW, Gutierrez T. 2017. Microbial extracellular polymeric substances (EPSs) in ocean systems. *Front Microbiol.* 8:922.
- Dreszer C, Vrouwenvelder JS, Paulitsch-Fuchs AH, Zwijnenburg A, Kruithof JC, Flemming HC. 2013. Hydraulic resistance of biofilms. *J Memb Sci.* 429:436–447.
- Erdinçler A, Vesilind PA. 2003. Effect of sludge water distribution on the liquid-solid separation of a biological sludge. *J Environ Sci Health A Tox Hazard Subst Environ Eng.* 38(10):2391–2400.
- Eselin J, Santos T, Hébraud M. 2018. Desiccation: an environmental and food industry stress that bacteria commonly face. *Food Microbiol.* 69:82–88.
- Fan LS, Leyva-Ramos R, Wisecarver KD, Zehner BJ. 1990. Diffusion of phenol through a biofilm grown on activated carbon particles in a draft-tube three-phase fluidized-bed bioreactor. *Biotechnol Bioeng.* 35(3):279–286.
- Feng J, Lamour G, Xue R, Mirvakli MN, Hatzikiriakos SG, Xu J, Li H, Wang S, Lu X. 2016. Chemical, physical and morphological properties of bacterial biofilms affect survival of encased *Campylobacter jejuni* F38011 under aerobic stress. *Int J Food Microbiol.* 238:172–182.
- Fernández-Delgado M, Duque Z, Rojas H, Suárez P, Contreras M, García-Amado MA. 2015. Environmental scanning electron microscopy analysis of *Proteus mirabilis* biofilms grown on chitin and stainless steel. *Ann Microbiol.* 65(3): 1401–1409.
- Fernández-Delgado M, Rojas H, Duque Z, Suárez P, Contreras M, García-Amado MA, Alciaturi C. 2016. Biofilm formation of *Vibrio cholerae* on stainless steel used in food processing. *Rev Inst Med Trop Sao Paulo.* 58(1):47.
- Flemming HC. 2008. In: Flemming HC, Murthy PS, Venkatesan R, editors. *Marine and industrial biofouling.* Berlin Heidelberg: Springer-Verlag.
- Flemming HC, Wingender J. 2010. The biofilm matrix. *Nat Rev Microbiol.* 8(9):623–633.
- Foerster K, Messiaen A-S, Raemdonck K, Nelis H, De Smedt S, Demeester J, Coenye T, Braeckmans K. 2014. Probing the size limit for nanomedicine penetration into Burkholderia multivorans and *Pseudomonas aeruginosa* biofilms. *J Control Release.* 195:21–28.
- Foster JS, Kolenbrander PE. 2004. Development of a multi-species oral bacterial community in a saliva-conditioned flow cell. *Appl Environ Microbiol.* 70(7):4340–4348.
- Galbiatti de Carvalho F, Puppim-Rontani RM, Portugal de Fucio SB, De Cassia Negrini T, Lemes Carlo H, Garcia-Godoy F. 2012. Analysis by confocal laser scanning microscopy of the MDPB bactericidal effect on *S. mutans* biofilm CLSM analysis of MDPB bactericidal effect on biofilm. *J Appl Oral Sci.* 20(5):568–575.
- Galdino RV, Benevides CA, Tenório RP. 2020. Diffusion maps of *Bacillus subtilis* biofilms via magnetic resonance imaging highlight a complex network of channels. *Colloids Surf B Biointerfaces.* 190:110905.
- Gantner S, Schmid M, Dürr C, Schuegger R, Steidle A, Hutzler P, Langebartels C, Eberl L, Hartmann A, Dazzo FB, et al. 2006. In situ quantitation of the spatial scale of calling distances and population density-independent N-acyl-homoserine lactone-mediated communication by rhizobacteria colonized on plant roots. *FEMS Microbiol Ecol.* 56(2):188–194.
- Gerbersdorf SU, Wieprecht S. 2015. Biostabilization of cohesive sediments: revisiting the role of abiotic conditions, physiology and diversity of microbes, polymeric secretion, and biofilm architecture. *Geobiology.* 13(1):68–97.
- Gusnaniar N, Sjollem J, Nuryastuti T, Peterson BW, van de Belt-Gritter B, de Jong ED, van der Mei HC, Busscher HJ. 2017. Structural changes in *S. epidermidis* biofilms after transmission between stainless steel surfaces. *Biofouling.* 33(9):712–721.
- Haisch C, Niessner R. 2007. Visualisation of transient processes in biofilms by optical coherence tomography. *Water Res.* 41(11):2467–2472.
- He Y, Peterson BW, Jongsma MA, Ren Y, Sharma PK, Busscher HJ, van der Mei HC. 2013. Stress relaxation analysis facilitates a quantitative approach towards antimicrobial penetration into biofilms. *PLoS One.* 8(5):e63750.
- He Y, Peterson BW, Ren Y, Van der Mei HC, Busscher HJ. 2014. Antimicrobial penetration in a dual-species oral biofilm after noncontact brushing: an in vitro study. *Clin Oral Investig.* 18(4):1103–1109.
- Herrling MP, Weisbrodt J, Kirkland CM, Williamson NH, Lackner S, Codd SL, Seymour JD, Guthausen G, Horn H. 2017. NMR investigation of water diffusion in different biofilm structures. *Biotechnol Bioeng.* 114(12):2857–2867.
- Hobley L, Ostrowski A, Rao FV, Bromley KM, Porter M, Prescott AR, MacPhee CE, van Aalten DMF, Stanley-Wall

- NR. 2013. BslA is a self-assembling bacterial hydrophobin that coats the *Bacillus subtilis* biofilm. *Proc Natl Acad Sci U S A*. 110(33):13600–13605.
- Hornemann JA, Codd SL, Fell RJ, Stewart PS, Seymour JD. 2009. Secondary flow mixing due to biofilm growth in capillaries of varying dimensions. *Biotechnol Bioeng*. 103(2):353–360.
- Hou J, Veeregowda DH, Van de Belt-Gritter B, Busscher HJ, Van der Mei HC. 2018. Extracellular polymeric matrix production and relaxation under fluid shear and mechanical pressure in *Staphylococcus aureus* biofilms. *Appl Environ Microbiol*. 84(1):e01516–17.
- Hou J, Wang C, Rozenbaum RT, Gusnaniar N, de Jong ED, Woudstra W, Geertsema-Doornbusch GI, Atema-Smit J, Sjollemma J, Ren Y, et al. 2019. Bacterial density and biofilm structure determined by optical coherence tomography. *Sci Rep*. 9(1):9794.
- Houry A, Gohar M, Deschamps J, Tischenko E, Aymerich S, Gruss A, Briandet R. 2012. Bacterial swimmers that infiltrate and take over the biofilm matrix. *Proc Natl Acad Sci U S A*. 109(32):13088–13093.
- Ivleva NP, Kubryk P, Niessner R. 2017. Raman microspectroscopy, surface-enhanced Raman scattering microspectroscopy, and stable-isotope Raman microspectroscopy for biofilm characterization. *Anal Bioanal Chem*. 409(18):4353–4375.
- Jafari M, Desmond P, Van Loosdrecht MCM, Derlon N, Morgenroth E, Picioreanu C. 2018. Effect of biofilm structural deformation on hydraulic resistance during ultrafiltration: a numerical and experimental study. *Water Res*. 145:375–387.
- Jones AAD, Buie CR. 2019. Continuous shear stress alters metabolism, mass-transport, and growth in electroactive biofilms independent of surface substrate transport. *Sci Rep*. 9(1):2602.
- Ju X, Chen J, Zhou M, Zhu M, Li Z, Gao S, Ou J, Xu D, Wu M, Jiang S, et al. 2020. Combating *Pseudomonas aeruginosa* biofilms by a chitosan-PEG-peptide conjugate via changes in assembled structure. *ACS Appl Mater Interfaces*. 12(12):13731–13738.
- Kim MK, Ingremeau F, Zhao A, Bassler BL, Stone HA. 2016. Local and global consequences of flow on bacterial quorum sensing. *Nat Microbiol*. 1(1):15005.
- Kundukad B, Seviour T, Liang Y, Rice SA, Kjelleberg S, Doyle PS. 2016. Mechanical properties of the superficial biofilm layer determine the architecture of biofilms. *Soft Matter*. 12(26):5718–5726.
- Laue H, Schenk A, Li H, Lambertsen L, Neu TR, Molin S, Ullrich MS. 2006. Contribution of alginate and levan production to biofilm formation by *Pseudomonas syringae*. *Microbiology*. 152(Pt 10):2909–2918.
- Lawrence JR, Wolfaardt GM, Korber DR. 1994. Determination of diffusion coefficients in biofilms by confocal laser microscopy. *Appl Environ Microbiol*. 60(4):1166–1173.
- Lei W, Krolla P, Schwartz T, Levkin PA. 2020. Controlling geometry and flow through bacterial bridges on patterned lubricant-infused surfaces (pLIS). *Small*. 16(52):2004575.
- Liu Y, Shi L, Van der Mei HC, Wu W, Ren Y, Busscher HJ. 2020. Perspectives on biomaterial-associated infection: pathogenesis and current clinical demands. In: Li B, Moriarty TF, Webster T, Xing M, editors. *Racing for the surface – pathogenesis of implant infection and advanced antimicrobial strategies*. Cham: Springer; p. 95–105.
- Luzar A, Chandler D. 1996. Hydrogen-bond kinetics in liquid water. *Nature*. 379(6560):55–57.
- Marks LR, Davidson BA, Knight PR, Hakansson AP. 2013. Interkingdom signaling induces *Streptococcus pneumoniae* biofilm dispersion and transition from asymptomatic colonization to disease. *MBio*. 4(4):e00438–13.
- Mattimore V, Battista JR. 1996. Radioresistance of *Deinococcus radiodurans*: functions necessary to survive ionizing radiation are also necessary to survive prolonged desiccation. *J Bacteriol*. 178(3):633–637.
- Oyebamiji OK, Wilkinson DJ, Jayathilake PG, Rushton SP, Bridgens B, Li B, Zuliani P. 2018. A Bayesian approach to modelling the impact of hydrodynamic shear stress on biofilm deformation. *PLoS One*. 13(4):e0195484.
- Panitz C, Frösler J, Wingender J, Flemming HC, Rettberg P. 2019. Tolerances of *Deinococcus geothermalis* biofilms and planktonic cells exposed to space and simulated martian conditions in low earth orbit for almost two years. *Astrobiology*. 19(8):979–994.
- Peterson BW, Busscher HJ, Sharma PK, Van der Mei HC. 2014. Visualization of microbiological processes underlying stress relaxation in *Pseudomonas aeruginosa* biofilms. *Microsc Microanal*. 20(3):912–915.
- Peterson BW, He Y, Ren Y, Zerdoum A, Libera MR, Sharma PK, van Winkelhoff A-J, Neut D, Stoodley P, van der Mei HC, et al. 2015. Viscoelasticity of biofilms and their recalcitrance to mechanical and chemical challenges. *FEMS Microbiol Rev*. 39(2):234–245.
- Peterson BW, Van der Mei HC, Sjollemma J, Busscher HJ, Sharma PK. 2013. A distinguishable role of eDNA in the viscoelastic relaxation of biofilms. *MBio*. 4(5):e00497–13.
- Phoenix VR, Holmes WM. 2008. Magnetic resonance imaging of structure, diffusivity, and copper immobilization in a phototrophic biofilm. *Appl Environ Microbiol*. 74(15):4934–4943.
- Piard JC, Kim SY, Deschamps J, Li Y, Dorel C, Gruss A, Trubuil A, Briandet R. in 2017. In: Flemming HC, Neu TR, Wingender J, editors. *The perfect slime: microbial extracellular polymeric substances*. London: IWA Press, p. 182.
- Qi Y, Thapa KB, Hoadley AFA. 2011. Application of filtration aids for improving sludge dewatering properties – a review. *Chem Eng J*. 171(2):373–384.
- Quan K, Zhang Z, Chen H, Ren X, Ren Y, Peterson BW, van der Mei HC, Busscher HJ. 2019. Artificial channels in an infectious biofilm created by magnetic nanoparticles enhanced bacterial killing by antibiotics. *Small*. 15(39):e1902313.
- Rani SA, Pitts B, Stewart PS. 2005. Rapid diffusion of fluorescent tracers into *Staphylococcus epidermidis* biofilms visualized by time lapse microscopy. *Antimicrob Agents Chemother*. 49(2):728–732.
- Rapoport A, Golovina EA, Gervais P, Dupont S, Beney L. 2019. Anhydrobiosis: inside yeast cells. *Biotechnol Adv*. 37(1):51–67.
- Rehl B, Gibbs JM. 2021. Role of ions on the surface-bound water structure at the silica/water interface: identifying the spectral signature of stability. *J Phys Chem Lett*. 12(11):2854–2864.
- Ren Y, Wang C, Chen Z, Allan E, Van der Mei HC, Busscher HJ. 2018. Emergent heterogeneous microenvironments in

- biofilms: substratum surface heterogeneity and bacterial adhesion force-sensing. *FEMS Microbiol Rev.* 42(3): 259–272.
- Renslow RS, Majors PD, McLean JS, Fredrickson JK, Ahmed B, Beyenal H. 2010. In situ effective diffusion coefficient profiles in live biofilms using pulsed-field gradient nuclear magnetic resonance. *Biotechnol Bioeng.* 106(6):928–937.
- Roberts ME, Stewart PS. 2004. Modeling antibiotic tolerance in biofilms by accounting for nutrient limitation. *Antimicrob Agents Chemother.* 48(1):48–52.
- Rooney LM, Amos WB, Hoskisson PA, McConnell G. 2020. Intra-colony channels in *E. coli* function as a nutrient uptake system. *ISME J.* 14(10):2461–2473.
- Rumbaugh KP, Sauer K. 2020. Biofilm dispersion. *Nat Rev Microbiol.* 18(10):571–586.
- Sandt C, Palmer TS, Pink J, Pink D. 2008. Quantification of local water and biomass in wild type PA01 biofilms by Confocal Raman Microspectroscopy. *J Microbiol Methods.* 75(1):148–152.
- Sandt C, Smith-Palmer T, Comeau J, Pink D. 2009. Quantification of water and biomass in small colony variant PA01 biofilms by confocal Raman microspectroscopy. *Appl Microbiol Biotechnol.* 83(6):1171–1182.
- Sandt C, Smith-Palmer T, Pink J, Brennan L, Pink D. 2007. Confocal Raman microspectroscopy as a tool for studying the chemical heterogeneities of biofilms in situ. *J Appl Microbiol.* 103(5):1808–1820.
- Sankaran J, Tan NJHJ, But KP, Cohen Y, Rice SA, Wohland T. 2019. Single microcolony diffusion analysis in *Pseudomonas aeruginosa* biofilms. *NPJ Biofilms Microbiomes.* 5(1):35.
- Seminara A, Angelini TE, Wilking JN, Vlamakis H, Ebrahim S, Kolter R, Weitz DA, Brenner MP. 2012. Osmotic spreading of *Bacillus subtilis* biofilms driven by an extracellular matrix. *Proc Natl Acad Sci U S A.* 109(4):1116–1121.
- Seymour JD, Codd SL, Gjersing EL, Stewart PS. 2004. Magnetic resonance microscopy of biofilm structure and impact on transport in a capillary bioreactor. *J Magn Reson.* 167(2):322–327.
- Sjollema J, Rustema-Abbing M, Van der Mei HC, Busscher HJ. 2011. Generalized relationship between numbers of bacteria and their viability in biofilms. *Appl Environ Microbiol.* 77(14):5027–5029.
- Stewart PS. 1998. A review of experimental measurements of effective diffusive permeabilities and effective diffusion coefficients in biofilms. *Biotechnol Bioeng.* 59(3):261–272.
- Stewart PS. 2003. Diffusion in biofilms. *J Bacteriol.* 185(5): 1485–1491.
- Stewart PS. 2012. Mini-review: convection around biofilms. *Biofouling.* 28(2):187–198.
- Stewart PS, Davison WM, Steenbergen JN. 2009. Daptomycin rapidly penetrates a *Staphylococcus epidermidis* biofilm. *Antimicrob Agents Chemother.* 53(8):3505–3507.
- Stewart PS, Rayner J, Roe F, Rees WM. 2001. Biofilm penetration and disinfection efficacy of alkaline hypochlorite and chlorosulfamates. *J Appl Microbiol.* 91(3):525–532.
- Stoodley P, Debeer D, Lewandowski Z. 1994. Liquid flow in biofilm systems. *Appl Environ Microbiol.* 60(8):2711–2716.
- Stoodley P, Hall-Stoodley L, Boyle JD, Jorgensen F, Lappin-Scott HM. 2000. In: Allison DG, Gilbert P, Lappin-Scott HM, Wilson M, editors. *Community structure and cooperation in biofilms.* Cambridge: Cambridge University Press; p. 53–64.
- Suci PA, Geesey GG, Tyler BJ. 2001. Integration of Raman microscopy, differential interference contrast microscopy, and attenuated total reflection Fourier transform infrared spectroscopy to investigate chlorhexidine spatial and temporal distribution in *Candida albicans* biofilms. *J Microbiol Methods.* 46(3):193–208.
- Suci PA, Mittelman MW, Yu FP, Geesey GG. 1994. Investigation of ciprofloxacin penetration into *Pseudomonas aeruginosa* biofilms. *Antimicrob Agents Chemother.* 38(9):2125–2133.
- Tam K, Kinsinger N, Ayala P, Qi F, Shi W, Myung NV. 2007. Real-time monitoring of *Streptococcus mutans* biofilm formation using a quartz crystal microbalance. *Caries Res.* 41(6):474–483.
- Tarek M, Tobias DJ. 2002. Role of protein-water hydrogen bond dynamics in the protein dynamical transition. *Phys Rev Lett.* 88(13):138101.
- Tolker-Nielsen T. 2015. Biofilm development. *Microbiol Spectr.* 3(2):MB–2014.
- Tzeng Y-L, Martin LE, Stephens DS. 2014. Environmental survival of *Neisseria meningitidis*. *Epidemiol Infect.* 142(1): 187–190.
- Van Leeuwenhoek A. 1684. An abstract of a letter from Mr. Anthony Leewenhoek at Delft, Dated Sep. 17. 1683. Containing some microscopical observations, about animals in the scurf of the teeth, the substance call'd worms in the nose, the cuticula consisting of scales. *Philos Trans R Soc.* 14:568.
- Van Oss CJ. 2003. Long-range and short-range mechanisms of hydrophobic attraction and hydrophilic repulsion in specific and aspecific interactions. *J Mol Recognit.* 16(4): 177–190.
- Van Oss CJ, Giese RF. 2005. Role of the properties and structures of liquid water in colloidal and interfacial systems. *J Dispers Sci Technol.* 25(5):631–655.
- Vogt M, Flemming HC, Veeman WS. 2000. Diffusion in *Pseudomonas aeruginosa* biofilms: a pulsed field gradient NMR study. *J Biotechnol.* 77(1):137–146.
- Vrouwenvelder JS, Dreszer C, Valladares Linares R, Kruihof JC, Mayer C, Flemming HC. 2017. In: Flemming HC, Neu TR, Wingender J, editors. *The perfect slime: microbial extracellular polymeric substances.* London: IWA Press; p. 193–206.
- Wagner M, Manz B, Volke F, Neu TR, Horn H. 2010. Online assessment of biofilm development, sloughing and forced detachment in tube reactor by means of magnetic resonance microscopy. *Biotechnol Bioeng.* 107(1):172–181.
- Waharte F, Steenkeste K, Briandet R, Fontaine-Aupart MP. 2010. Diffusion measurements inside biofilms by image-based fluorescence recovery after photobleaching (FRAP) analysis with a commercial confocal laser scanning microscope. *Appl Environ Microbiol.* 76(17):5860–5869.
- Wang C, Hou J, Van der Mei HC, Busscher HJ, Ren Y. 2019. Emergent properties in *Streptococcus mutans* biofilms are controlled through adhesion force sensing by initial colonizers. *MBio.* 10(5):e01908–19.
- Webb JS, Thompson LS, James S, Charlton T, Tolker-Nielsen T, Koch B, Givskov M, Kjelleberg S. 2003. Cell death in *Pseudomonas aeruginosa* biofilm development. *J Bacteriol.* 185(15):4585–4592.

- Wei H, Gao B, Ren J, Li A, Yang H. 2018. Coagulation/flocculation in dewatering of sludge: a review. *Water Res.* 143(2015):608–631.
- Wilking JN, Zaburdaev V, De Volder M, Losick R, Brenner MP, Weitz DA. 2013. Liquid transport facilitated by channels in *Bacillus subtilis* biofilms. *Proc Natl Acad Sci USA.* 110(3): 848–852.
- Williamson K, McCarty PL. 1976. Verification studies of the biofilm model for bacterial substrate utilization. *J Water Pollut Control Fed.* 48(2):281–296.
- Wilson C, Lukowicz R, Merchant S, Valquier-Flynn H, Caballero J, Sandoval J, et al. 2017. Quantitative and qualitative assessment methods for biofilm growth: a mini-review. *Res Rev J Eng Technol.* 6(4):1–25.
- Wood BD, Quintard M, Whitaker S. 2002. Calculation of effective diffusivities for biofilms and tissues. *Biotechnol Bioeng.* 77(5):495–516.
- Wu B, Dai X, Chai X. 2020. Critical review on dewatering of sewage sludge: influential mechanism, conditioning technologies and implications to sludge re-utilizations. *Water Res.* 180:115912.
- Xu Q, Huang QS, Wei W, Sun J, Dai X, Ni BJ. 2020. Improving the treatment of waste activated sludge using calcium peroxide. *Water Res.* 187:116440.
- Yan J, Nadell CD, Stone HA, Wingreen NS, Bassler BL. 2017. Extracellular-matrix-mediated osmotic pressure drives *Vibrio cholerae* biofilm expansion and cheater exclusion. *Nat Commun.* 8(1):327.
- Yang J, Evans BA, Rozen DE. 2010. Signal diffusion and the mitigation of social exploitation in pneumococcal competence signalling. *Proc Biol Sci.* 277(1696):2991–2999.
- Zhang X, Bishop PL, Kupferle MJ. 1998. Measurement of polysaccharides and proteins in biofilm extracellular polymers. *Water Sci Technol.* 37(4–5):345–348.
- Zhang C, Li X, Wang Z, Huang X, Ge Z, Hu B. 2020. Influence of structured water layers on protein adsorption process: a case study of cytochrome c and carbon nanotube interactions and its implications. *J Phys Chem B.* 124(4):684–694.
- Zhang X, Zhou X, Xi H, Sun J, Liang X, Wei J, Xiao X, Liu Z, Li S, Liang Z, et al. 2019. Interpretation of adhesion behaviors between bacteria and modified basalt fiber by surface thermodynamics and extended DLVO theory. *Colloids Surf B Biointerfaces.* 177(301):454–461.
- Zhou L, Zhang LH, Cámara M, He YW. 2017. The DSF family of quorum sensing signals: diversity, biosynthesis, and turnover. *Trends Microbiol.* 25(4):293–303.
- Zhu F, Jiang H, Zhang Z, Zhao L, Wang J, Hu J, Zhang H. 2012. Research on drying effect of different additives on sewage sludge. *Procedia Environ Sci.* 16:357–362.